

JET PROPULSION LABORATORY

SIRTF IPF REPORT

JPL ID504087

December 4, 2003

**SIRTF INSTRUMENT POINTING FRAME
KALMAN FILTER EXECUTION SUMMARY**

IPF RUN NUMBER: 504087

REPORT TYPE: IOC EXECUTION (FINE)

PRIME FRAME: MIPS_160um_center_large_FOV (87)

INFERRRED FRAMES: (88) (89) (91) (92)

IPF TEAM

Autonomy and Control Section (345)

Jet Propulsion Laboratory

California Institute of Technology

4800 Oak Grove Drive

Pasadena, CA 91109

Contents

1 IPF EXECUTION SUMMARY	5
2 IPF INPUT FILE HISTORY	9
3 IPF EXECUTION RESULTS	13
3.1 IPF EXECUTION OUTPUT PLOTS	13
3.2 IPF OUTPUT DATA (IF MINI FILE)	39
3.3 IPF EXECUTION LOG	42
4 COMMENTS	46

List of Figures

1.1 A-priori and a-posteriori IPF frames	5
1.2 A-priori and a-posteriori IPF frames (ZOOMED)	8
2.1 Scenario Plot	9
2.2 Attitude file edit history	10
2.3 Centroid file edit history	11
2.4 Oriented Pixel Coords of Centroid Meas. Edited Centroids	12
3.1 TPF coords of measurements and a-priori predicts	15
3.2 Oriented Pixel Coords of measurements and a-priori predicts	15
3.3 Oriented (W,V) Pixel Coords of A-Priori Prediction Error Quiver Plot	16
3.4 A-priori prediction error (Science Centroids)	16
3.5 Oriented Pixel Coords of measurements and a-priori predicts (PCRS only)	17
3.6 Oriented Pixel Coords of measurements and a-priori predicts (Zoomed, PCRS only)	17
3.7 Oriented (W,V) Pixel Coords of A-Priori PCRS Prediction Error Quiver Plot	18
3.8 A-priori PCRS prediction error	18
3.9 IPF execution convergence, chart 1	19
3.10 IPF execution convergence, chart 2	19
3.11 Parameter uncertainty convergence	20
3.12 IPF parameter symbol table	20

3.13 KF parameter error sigma plots	21
3.14 LS parameter error sigma plot	21
3.15 KF and LS parameter error sigma plot	22
3.16 Oriented Pixel Coords of meas. and a-posteriori predicts	23
3.17 Oriented Pixel Coords of meas. and a-posteriori predicts (attitude corrected)	23
3.18 KF innovations with (o) and w/o (+) attitude corrections	24
3.19 Histograms of science a-posteriori residuals (or innovations)	24
3.20 A-Posteriori Science Centroid Prediction Error Quiver (Att. Cor.)	25
3.21 Normalized A-Posteriori Science Centroid Prediction Errors	25
3.22 KF innovations with (o) and w/o (+) attitude corrections (PCRS)	26
3.23 Histograms of PCRS a-posteriori residuals (or innovations)	26
3.24 A-posteriori PCRS Prediction Summary	27
3.25 A-posteriori PCRS Prediction (PCRS 1 Only)	28
3.26 A-posteriori PCRS Prediction (PCRS 2 Only)	28
3.27 A-Posteriori PCRS Prediction Errors Quiver (Att. Cor.)	29
3.28 Normalized A-Posteriori PCRS Prediction Errors	29
3.29 W-axis KF innovations and 1-sigma bound	30
3.30 V-axis KF innovations and 1-sigma bound	30
3.31 Array plot with (solid) and w/o (dashed) optical distortion corrections	31
3.32 Optical Distortion Plot: total (x5 magnification)	31
3.33 Optical Distortion Plot: constant plate scales (x5 magnification)	32
3.34 Optical Distortion Plot: linear plate scale (x5 magnification)	32
3.35 Optical Distortion Plot: gamma terms (x5 magnification)	33
3.36 Scan Mirror Chops	33
3.37 IPF Frame Reconstruction	34
3.38 Center Pixel Reconstruction	34
3.39 Estimated attitude corrections (Body frame)	35
3.40 Estimated attitude error sigma plot (Body frame)	35
3.41 Thermo-mechanical boresight drift (equiv. angle in (W,V) coords)	36
3.42 Thermo-mechanical boresight drift (equiv. angle in Body frame)	36
3.43 Gyro drift bias contribution (equiv. rate in (W,V) coords)	37

3.44	Gyro drift bias contribution (equiv. angle in (W,V) coords)	37
3.45	Gyro drift bias contribution (equiv. angle in Body frame)	38

List of Tables

1.1	IPF filter input files	6
1.2	IPF filter execution configuration	6
1.3	IPF filter execution mask vector assignment	6
1.4	IPF calibration error summary ([arcsec], 1-sigma, radial)	7
1.5	Science measurement prediction error summary (1-sigma)	7
1.6	IPF Brown angle summary	8
2.1	IPF input file begin and end times	9
2.2	IPF input file editing status	9
2.3	List of Removed Centroids (Original CA File Row Index)	12
2.4	List of Removed PCRS Centroids (Original CB File Row Index)	12
3.1	Table of figures I (IPF run)	13
3.2	Table of figures II (IPF run)	14
3.3	PCRS measurement prediction error summary	27

1 IPF EXECUTION SUMMARY

This report summarizes the SIRTF Instrument Pointing Frame (IPF) Kalman Filter execution associated with run file: RN504087. In particular, this Focal Point Survey calibrates the instrument: MIPS_160um_center_large_FOV (87), as part of the IOC Fine Survey. The main calibration results from the IPF filter execution have been documented in IF504087 typically stored in the mission archive DOM collection IPF_IF. This report only summarizes the main aspects of the run, and does not substitute for the full information contained in the IF file.

Section 1 summarizes the filter execution results. The filter configurations are tabulated in Table 1.2 and the mask vector assignments are tabulated in Table 1.3. A total of 22 state parameters are estimated in this run. The overall End-to-End pointing performances are tabulated in Table 1.4. The prediction residuals throughout the estimation processes are tabulated in Table 1.5. Section 3 summarizes resulting plots, a mini summary of the IF IPF output file, and the execution log. Section 4 captures the user comments that are specific to this particular run.

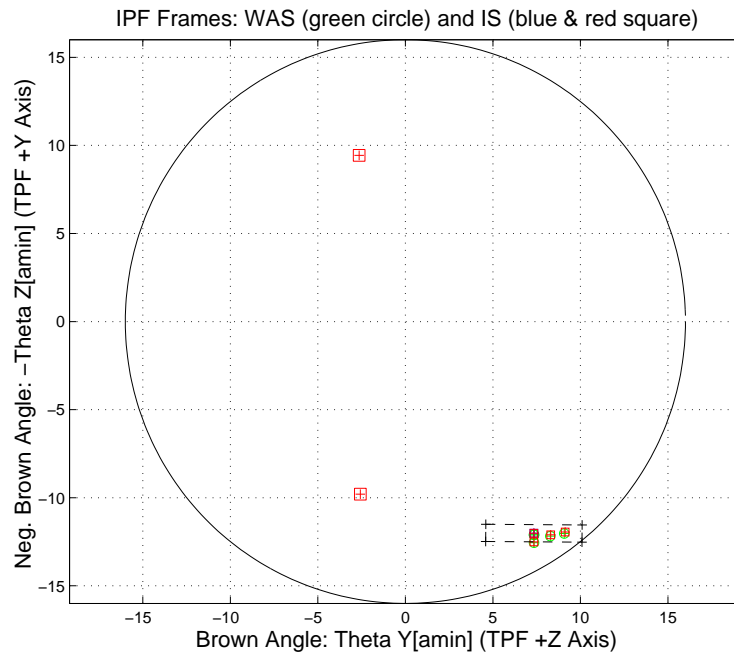


Figure 1.1: A-priori and a-posteriori IPF frames

RAW	FINAL (After Editing)
AA501087	AA501087
AS501087	AS501087
CA502087	CA502087
CB502087	CB901087
CS502087	CS502087

Table 1.1: IPF filter input files

EXECUTION CONFIGURATION ITEM	CURRENT STATUS
IPF Filter Version Used	IPF.V3.0.0B
Frame Table Version Used	BodyFrames_FTU_14a
Scan-Mirror Employed?	YES
IPF Filter Mode	NORMAL-MODE(0)
SLIT-MODE Operation	DISABLED
Kalman Filter Operation	ENABLED
Least-Squares Data Analysis	ENABLED
IBAD Screening	DISABLED
User-Specified Data Editing	DISABLED
Total Number of Iterations	30
LS Residual Sigma Scale	5.73186553E-001
Total Number of Maneuvers	39

Table 1.2: IPF filter execution configuration

Con. Plate Scale			Γ Dependent				Γ^2 Dependent				Linear Plate Scale						Mirror	
a_{00}	b_{00}	c_{00}	a_{10}	b_{10}	c_{10}	d_{10}	a_{20}	b_{20}	c_{20}	d_{20}	a_{01}	b_{01}	c_{01}	d_{01}	e_{01}	f_{01}	α	β
1	2	3	4	5	6	7	8	9	10	11	12	13	14	15	16	17	18	19
1	1	0	0	0	0	0	0	0	0	0	0	0	0	0	0	0	1	1
IPF (T)			Alignment R						Gyro Drift Bias									
θ_1	θ_2	θ_3	a_{rx}	a_{ry}	a_{rz}	b_{rx}	b_{ry}	b_{rz}	c_{rx}	c_{ry}	c_{rz}	b_{gx}	b_{gy}	b_{gz}	c_{gx}	c_{gy}	c_{gz}	
20	21	22	23	24	25	26	27	28	29	30	31	32	33	34	35	36	37	
1	1	1	1	1	1	1	1	1	1	1	1	1	1	1	1	1	1	

Table 1.3: IPF filter execution mask vector assignment

FOCAL PLANE SURVEY ANALYSIS: IOC Fine Survey.

INSTRUMENT NAME: MIPS_160um_center_large_FOV NF: 87

PIX2RADW: 7.80550030E-005 [rad/pixel] = 1.6100E+001 [arcsec/pixel]

PIX2RADV: 7.80550030E-005 [rad/pixel] = 1.6100E+001 [arcsec/pixel]

FRAME	DESCRIPTION	IPF ¹	SF ²	TOTAL	REQ
087(P)	MIPS_160um_center_large_FOV	0.3594	0.0855	0.3694	3.70
088(I)	MIPS_160um_plusY_edge	0.4697	0.0855	0.4774	N/A
089(I)	MIPS_160um_large_only	0.3594	0.0855	0.3694	N/A
091(I)	MIPS_160um_small_FOV1	0.5640	0.0855	0.5704	N/A
092(I)	MIPS_160um_small_FOV2	0.4389	0.0855	0.4472	N/A

Table 1.4: IPF calibration error summary ([arcsec], 1-sigma, radial)

RMS METRIC	A PRIORI ³	A POSTERIORI ³	ATT. CORRECTED ⁴	UNITS
Radial	4.4575	2.9725	2.9646	arcsec
W-Axis	2.0224	1.9130	1.9010	arcsec
V-Axis	3.9723	2.2751	2.2749	arcsec
Radial	0.2769	0.1846	0.1841	pixels
W-Axis	0.1256	0.1188	0.1181	pixels
V-Axis	0.2467	0.1413	0.1413	pixels

Table 1.5: Science measurement prediction error summary (1-sigma)

¹IPF filter removes systematic pointing errors due to: thermomechanical alignment drift (Body to TPF), gyro bias and bias drift, centroiding error, attitude error, and optical distortion. IPF SIGMA presented here is “Scaled” by the Least Squares Scale factor. The Least Squares Scale Factor was: 0.573187. It is assumed that the gyro Angle Random Walk contribution is captured with the Least Squares scaling. The gyro ARW contribution can be approximately calculated as 0.0330 arcseconds, given that ARW = 100 $\mu\text{deg}/\sqrt{\text{hr}}$, with 5.885000e+002 second Maneuver time (max), and 39 independent Maneuvers.

²Gyro Scale Factor(GSF) assumes 95 ppm error over 0.250 degree maneuver.

³This can be interpreted as estimate of ”pixel to sky” pointing reconstruction error if no science data is used.

⁴This can be interpreted as estimate of achieved S/I centroiding error

IPF BROWN ANGLE SUMMARY					
FRAME TABLE USED: BodyFrames_FTU_14a					
NF	NAME	WAS	IS	CHANGE	UNIT
087	theta_Y	+7.347515	+7.341460	-0.006055	arcmin
087	theta_Z	+12.105588	+12.017026	-0.088562	arcmin
087	angle	+0.000006	+0.384662	+0.384656	deg
088	theta_Y	+7.347515	+7.338177	-0.009337	arcmin
088	theta_Z	+12.554659	+12.505950	-0.048708	arcmin
088	angle	+0.000006	+0.384662	+0.384656	deg
089	theta_Y	+7.347515	+7.341460	-0.006055	arcmin
089	theta_Z	+12.105588	+12.017026	-0.088562	arcmin
089	angle	+0.000006	+0.384662	+0.384656	deg
091	theta_Y	+9.077043	+9.130996	+0.053954	arcmin
091	theta_Z	+12.030743	+11.947549	-0.083194	arcmin
091	angle	+0.000006	+0.384662	+0.384656	deg
092	theta_Y	+8.278799	+8.304215	+0.025416	arcmin
092	theta_Z	+12.180433	+12.104981	-0.075452	arcmin
092	angle	+0.000006	+0.384662	+0.384656	deg

Table 1.6: IPF Brown angle summary

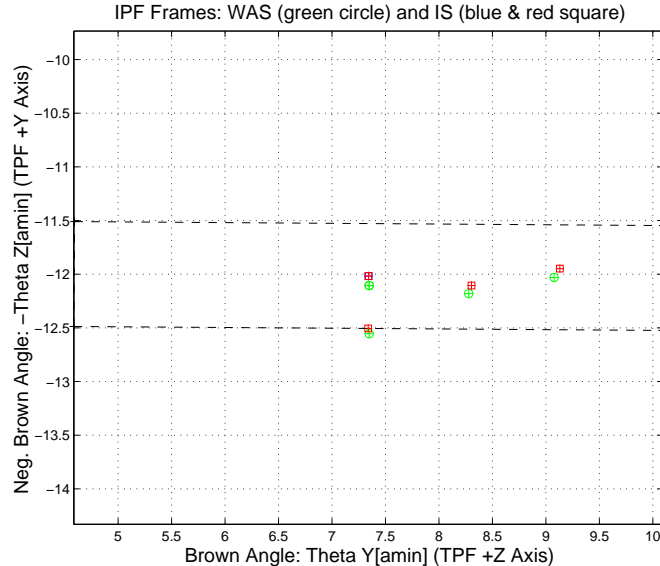


Figure 1.2: A-priori and a-posteriori IPF frames (ZOOMED)

2 IPF INPUT FILE HISTORY

STATUS	FILENAME	START TIME	END TIME
WAS	AA501087	752744000.3	752773000.4
IS	AA501087	752744000.3	752773000.4
WAS	CA502087	752745151.5	752772087.5
IS	CA502087	752745151.5	752772087.5
WAS	CB502087	752744913.3	752772305.4
IS	CB901087	752744913.3	752772305.4

Table 2.1: IPF input file begin and end times

WAS	SIZE	IS	SIZE	REMOVED	PATCHED
AA501087	290002	AA501087	290002	0	0
CA502087	100	CA502087	100	0	N/A
CB502087	180	CB901087	178	2	N/A

Table 2.2: IPF input file editing status

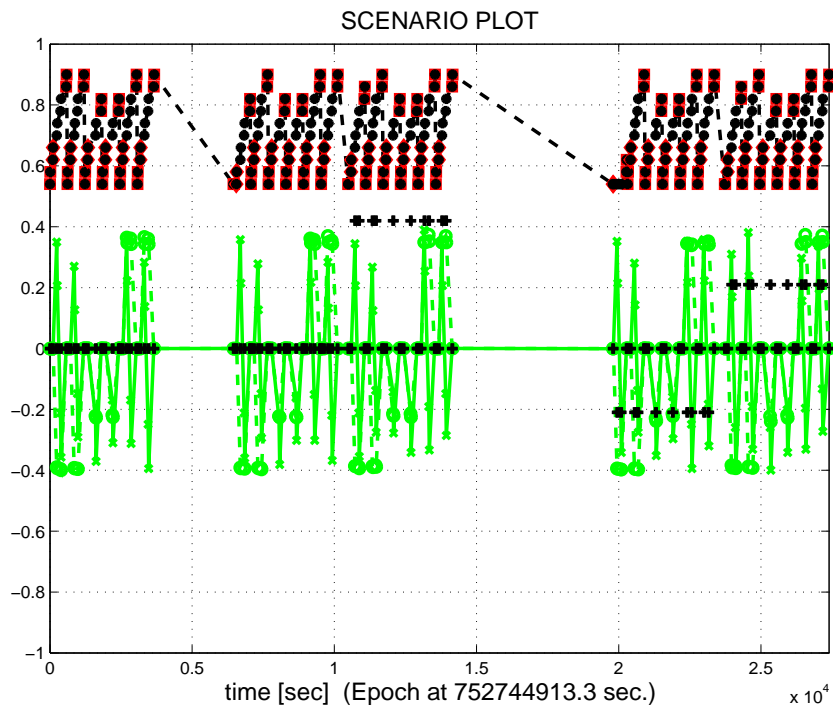


Figure 2.1: Scenario Plot

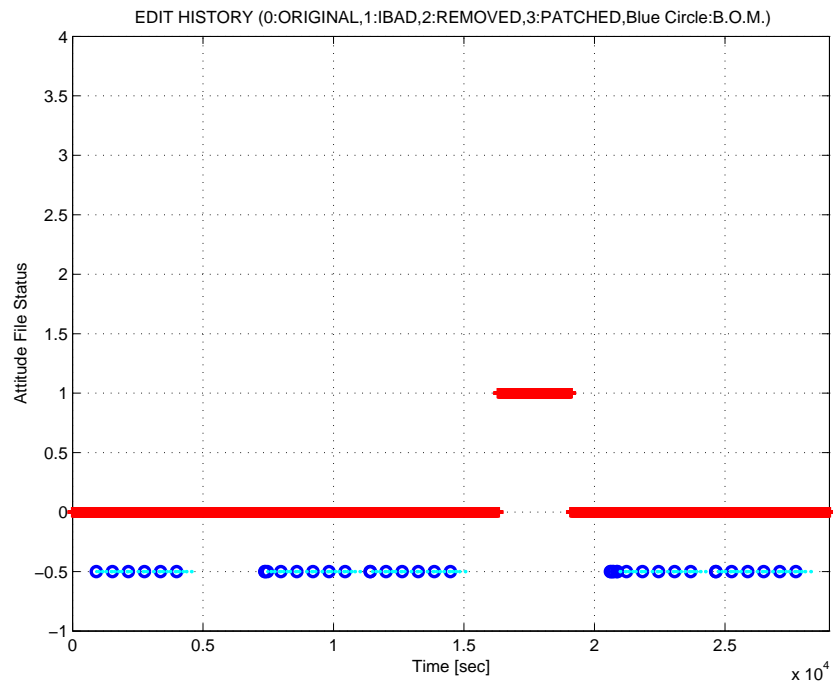


Figure 2.2: Attitude file edit history

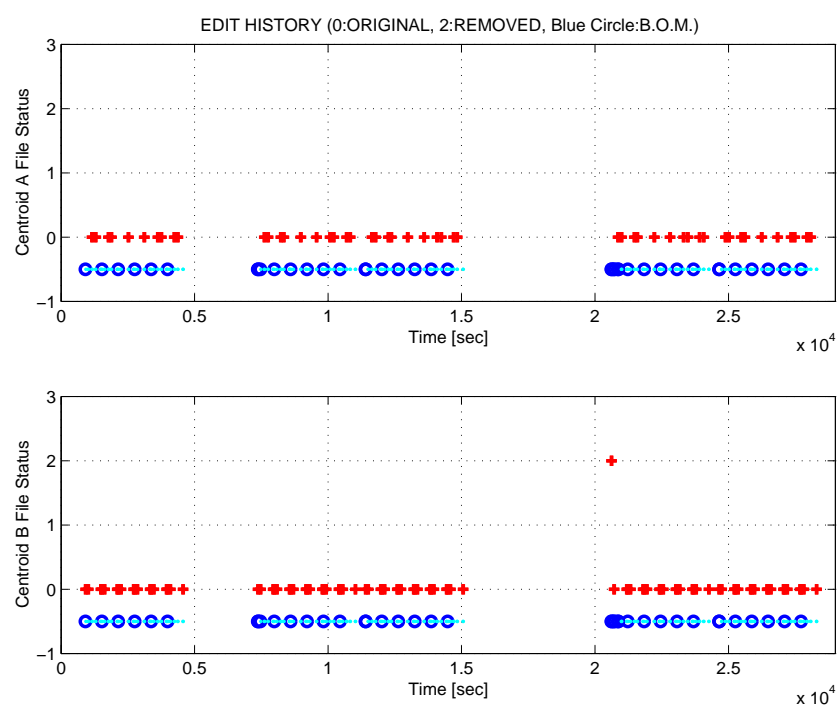


Figure 2.3: Centroid file edit history

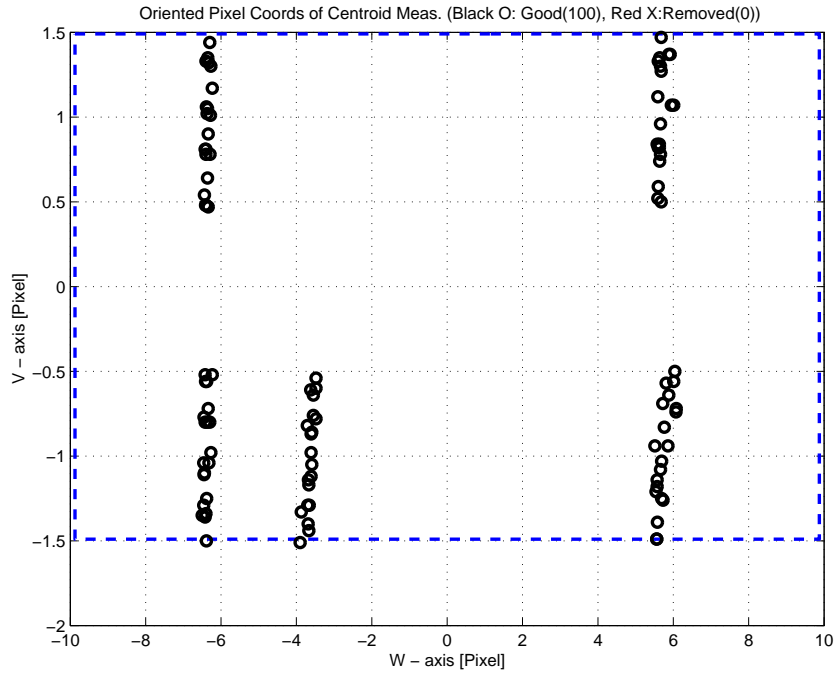


Figure 2.4: Oriented Pixel Coords of Centroid Meas. Edited Centroids

LIST OF REMOVED SCIENCE CENTROIDS

Table 2.3: List of Removed Centroids (Original CA File Row Index)

LIST OF REMOVED PCRS CENTROIDS									
--------------------------------	--	--	--	--	--	--	--	--	--

109	110								
-----	-----	--	--	--	--	--	--	--	--

Table 2.4: List of Removed PCRS Centroids (Original CB File Row Index)

3 IPF EXECUTION RESULTS

3.1 IPF EXECUTION OUTPUT PLOTS

This subsection summarizes the IPF filter results. As shown in Table 3.1, the output plots are segmented to three groups: predicted performance, post-run results and IPF trending plots.

FIGURE NO.	DESCRIPTION
Predicted performance prior to IPF run	
Figure 3.1	Meas. and a-priori predicts in TPF coords
Figure 3.2	Meas. and a-priori predicts in Oriented Pixel Coords including rectangular array boundary approximation
Figure 3.3	A-Priori Prediction Error Quiver Plot in Oriented Pixel Coords including rectangular array boundary approximation
Figure 3.4	A-priori prediction error
Figure 3.5	Oriented Pixel Coords of measurements and a-priori predicts (PCRS only)
Figure 3.6	Oriented Pixel Coords of measurements and a-priori predicts (Zoomed, PCRS only)
Figure 3.7	Oriented (W,V) Pixel Coords of A-Priori PCRS Prediction Error Quiver Plot
Figure 3.8	A-priori PCRS prediction error
IPF filter performance (post run results)	
Figure 3.9	IPF execution convergence, chart 1: (top) normalized residual error vs. iteration number and (bottom) norm of effective parameter corrections
Figure 3.10	IPF execution convergence, chart 2: parameter correction size vs. iteration number
Figure 3.11	Parameter uncertainty convergence: square-root of diagonal elements of covariance matrix vs. maneuver number
Figure 3.12	IPF parameter symbol table
Figure 3.13	KF parameter error sigma plot (a-priori-dashed, a-posteriori-solid). Includes true parameter errors (FLUTE runs only)
Figure 3.14	LS parameter error sigma plot. Includes true parameter errors (FLUTE runs only)
Figure 3.15	KF and LS parameter errors sigma plot (Figure 3.13 & Figure 3.14 combined)
Figure 3.16	Measurements and a-posteriori predicts in Oriented Pixel Coords including rectangular array boundaries (a-priori-dashed, a-posteriori-solid)
Figure 3.17	Attitude corrected meas. and a-posteriori predicts in Oriented Pixel Coords including rectangular array boundaries (a-priori-dashed, a-posteriori-solid)

Table 3.1: Table of figures I (IPF run)

FIGURE NO.	DESCRIPTION
IPF filter performance (post run results) - CONTINUE	
Figure 3.18	KF innovations with (o) and w/o (+) attitude corrections
Figure 3.19	Histograms of science a-posteriori residuals (or innovations)
Figure 3.20	A-Posteriori Science Centroid Prediction Error Quiver (Att. Cor.)
Figure 3.21	Normalized A-Posteriori Science Centroid Prediction Errors
Figure 3.22	KF innovations with (o) and w/o (+) attitude corrections (PCRS)
Figure 3.23	Histograms of PCRS a-posteriori residuals (or innovations)
Figure 3.24	A-posteriori PCRS Prediction Summary
Figure 3.25	A-posteriori PCRS Prediction (PCRS 1 Only)
Figure 3.26	A-posteriori PCRS Prediction (PCRS 2 Only)
Figure 3.27	A-Posteriori PCRS Prediction Errors Quiver (Att. Cor.)
Figure 3.28	Normalized A-Posteriori PCRS Prediction Errors
Figure 3.29	W-axis KF innovations and 1-sigma bound
Figure 3.30	V-axis KF innovations and 1-sigma bound
Figure 3.31	Array plot with (solid) and w/o (dashed) optical distortion corrections
Figure 3.32	Optical Distortion Plot: total (x5 magnification)
Figure 3.33	Optical Distortion Plot: constant plate scales (x5 magnification)
Figure 3.34	Optical Distortion Plot: linear plate scale (x5 magnification)
Figure 3.35	Optical Distortion Plot: gamma terms (x5 magnification)
Figure 3.36	Scan Mirror Chops
Figure 3.37	IPF Frame Reconstruction
Figure 3.38	Center Pixel Reconstruction
IPF parameter trending plots	
Figure 3.39	Estimated attitude corrections (Body frame)
Figure 3.40	Estimated attitude error sigma plot (Body frame)
Figure 3.41	Systematic error attributed to thermo-mechanical boresight drift (equiv. angle in (W,V) coords)
Figure 3.42	Systematic error attributed to thermo-mechanical boresight drift (equiv. angle in Body frame)
Figure 3.43	Systematic error attributed to gyro drift bias (equiv. rate in (W,V) coords)
Figure 3.44	Systematic error attributed to gyro drift bias (equiv. angle in (W,V) coords)
Figure 3.45	Systematic error attributed to gyro drift bias (equiv. angle in Body frame)

Table 3.2: Table of figures II (IPF run)

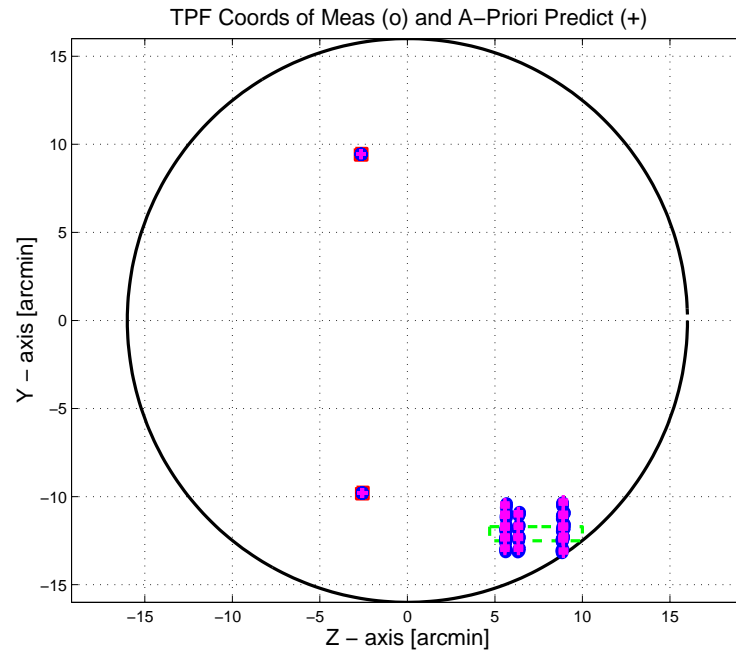


Figure 3.1: TPF coords of measurements and a-priori predicts

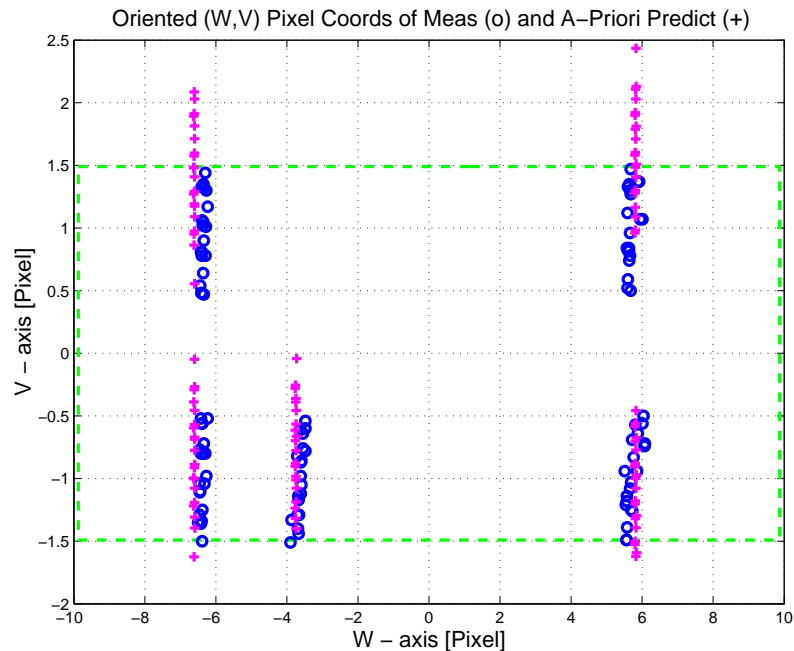


Figure 3.2: Oriented PixelCoords of measurements and a-priori predicts

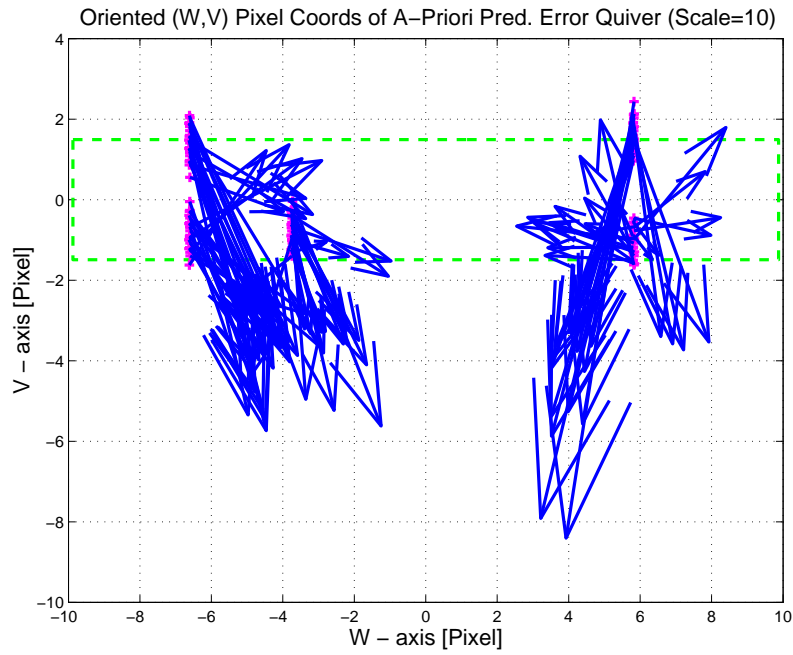


Figure 3.3: Oriented (W,V) Pixel Coords of A-Priori Prediction Error Quiver Plot

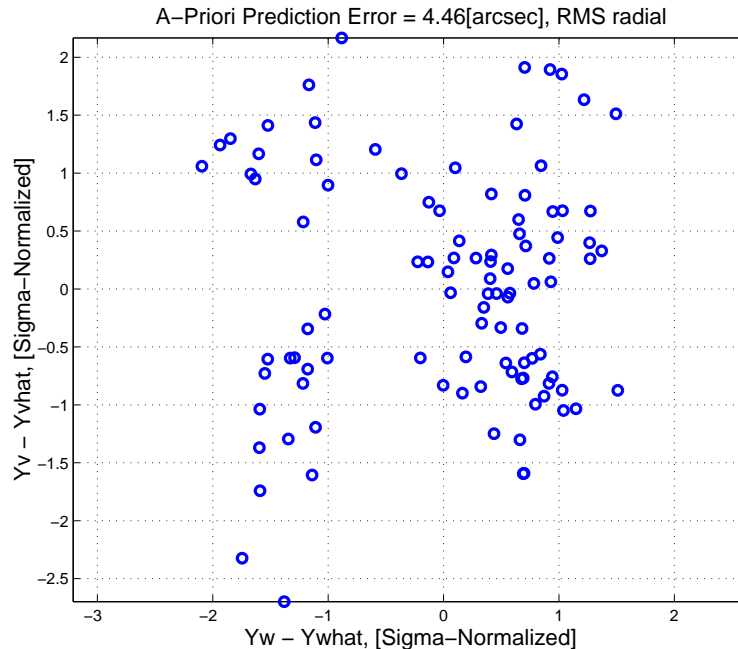


Figure 3.4: A-priori prediction error (Science Centroids)

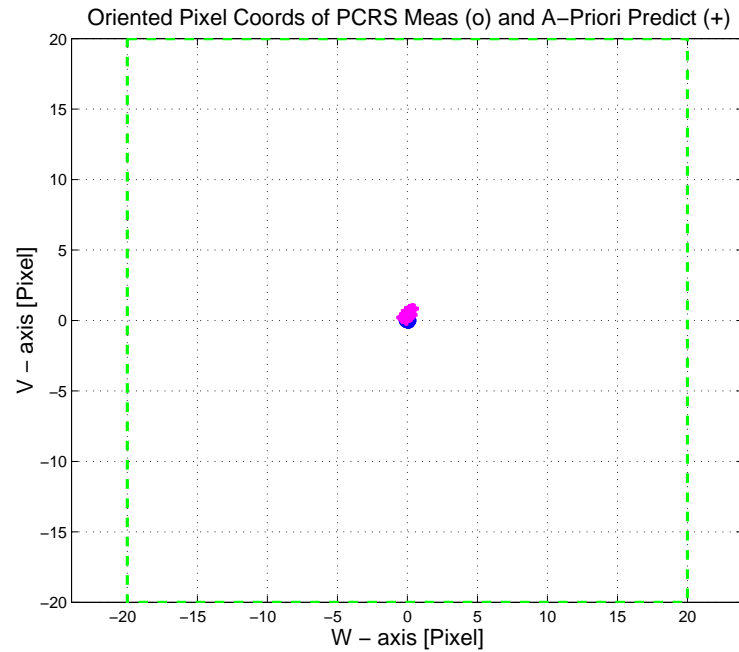


Figure 3.5: Oriented Pixel Coords of measurements and a-priori predicts (PCRS only)

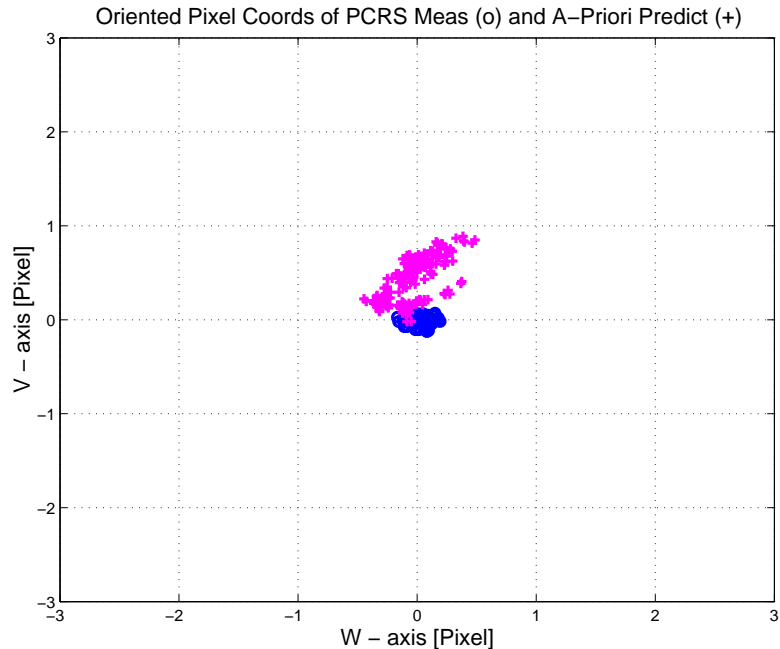


Figure 3.6: Oriented Pixel Coords of measurements and a-priori predicts (Zoomed, PCRS only)

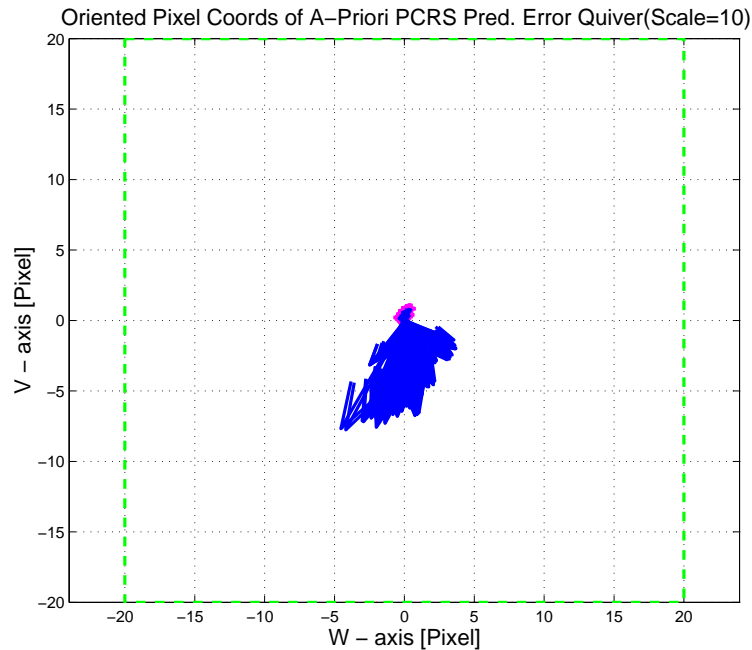


Figure 3.7: Oriented (W,V) Pixel Coords of A-Priori PCRS Prediction Error Quiver Plot

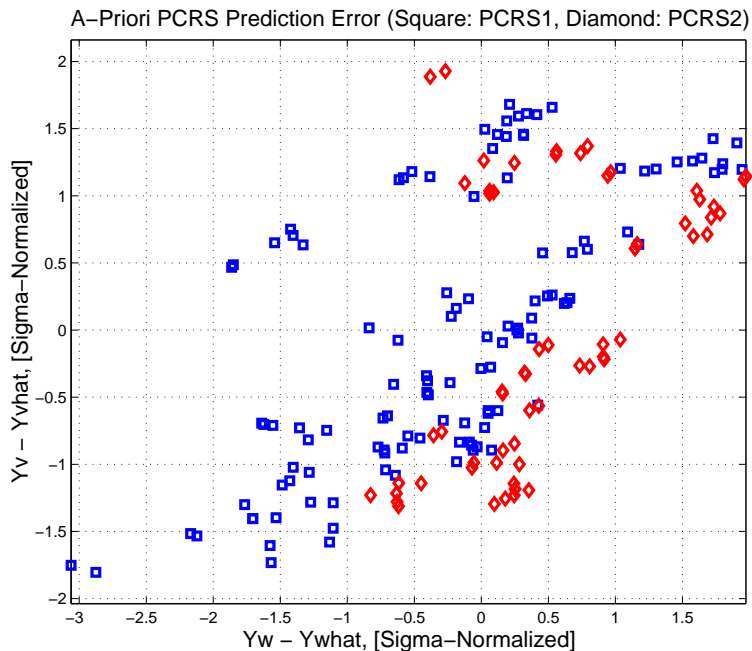


Figure 3.8: A-priori PCRS prediction error

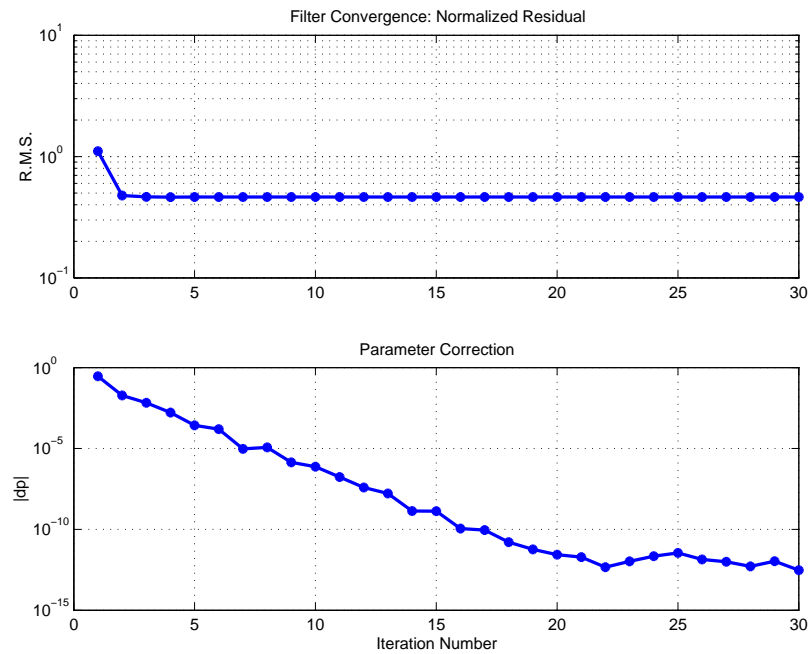


Figure 3.9: IPF execution convergence, chart 1

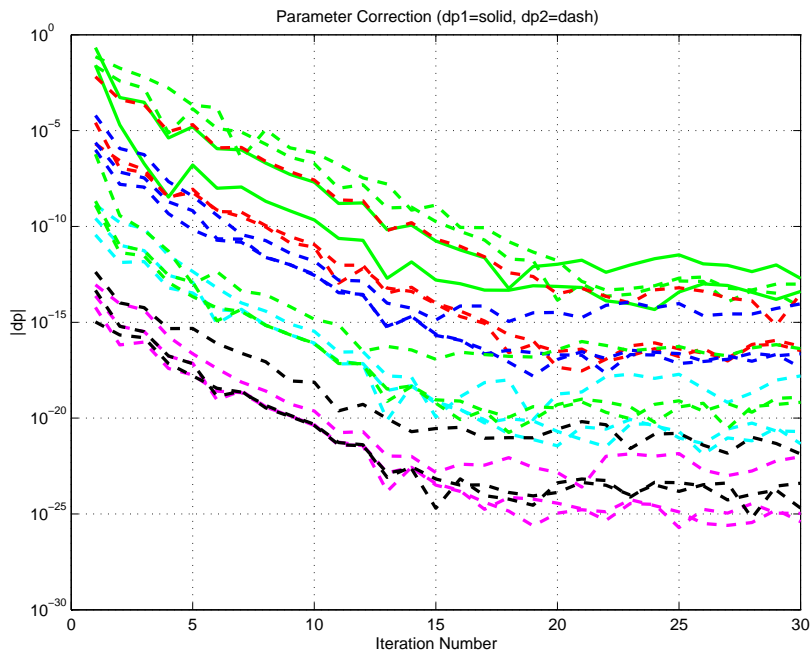


Figure 3.10: IPF execution convergence, chart 2

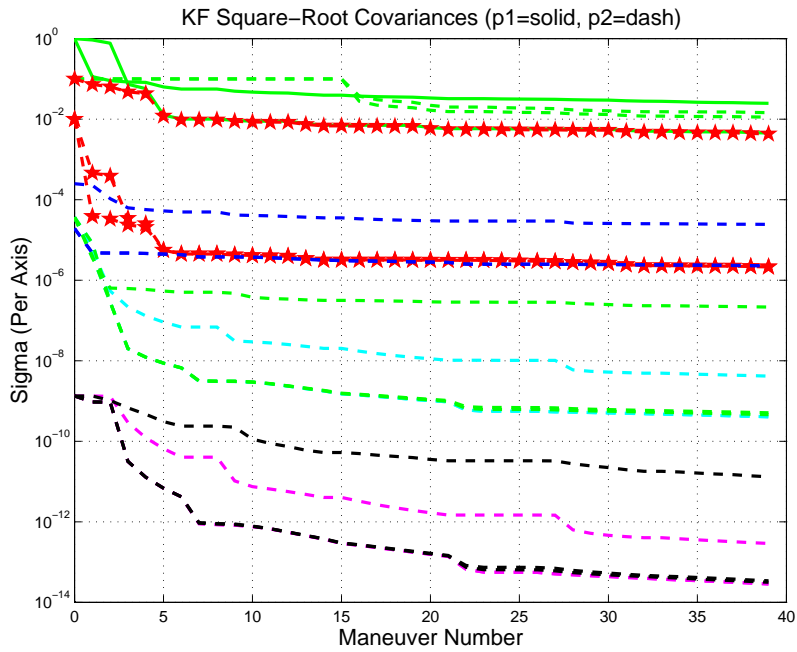


Figure 3.11: Parameter uncertainty convergence

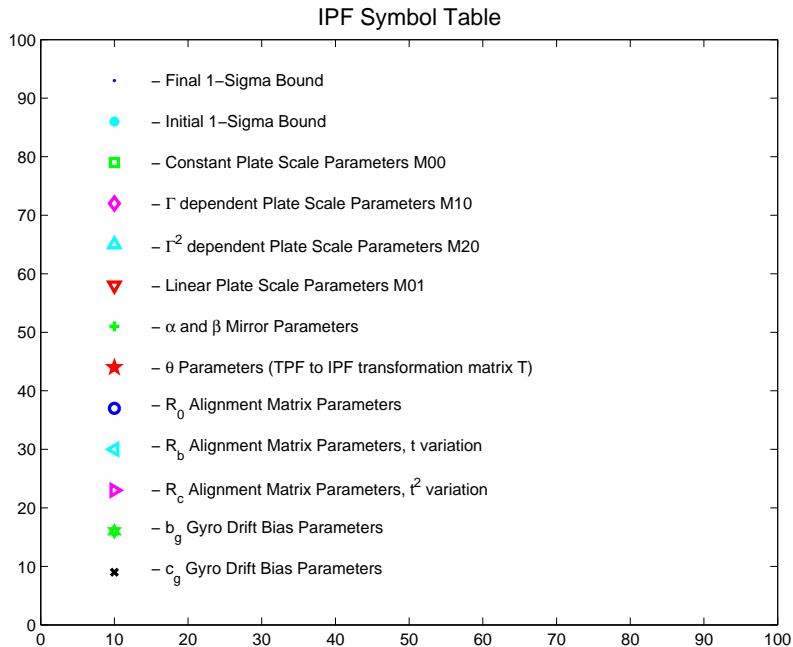


Figure 3.12: IPF parameter symbol table

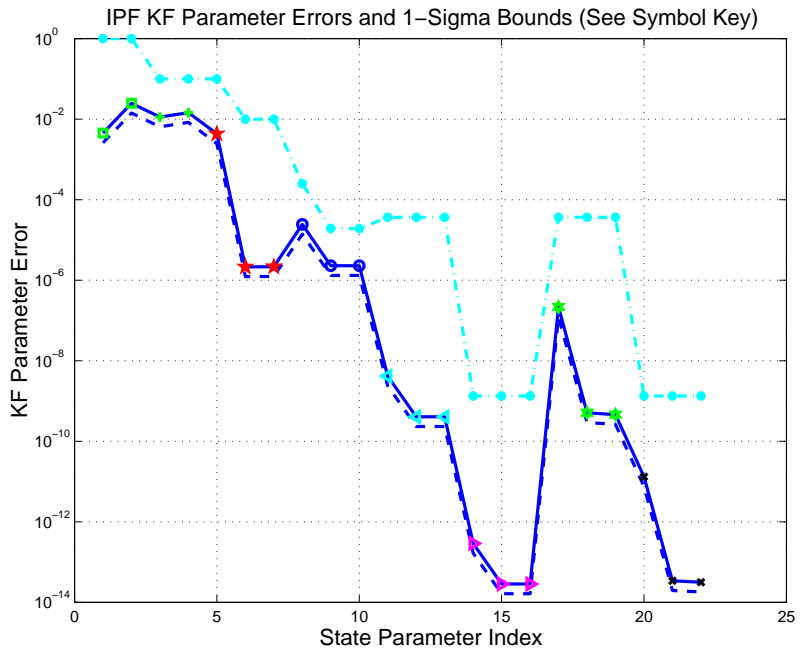


Figure 3.13: KF parameter error sigma plots

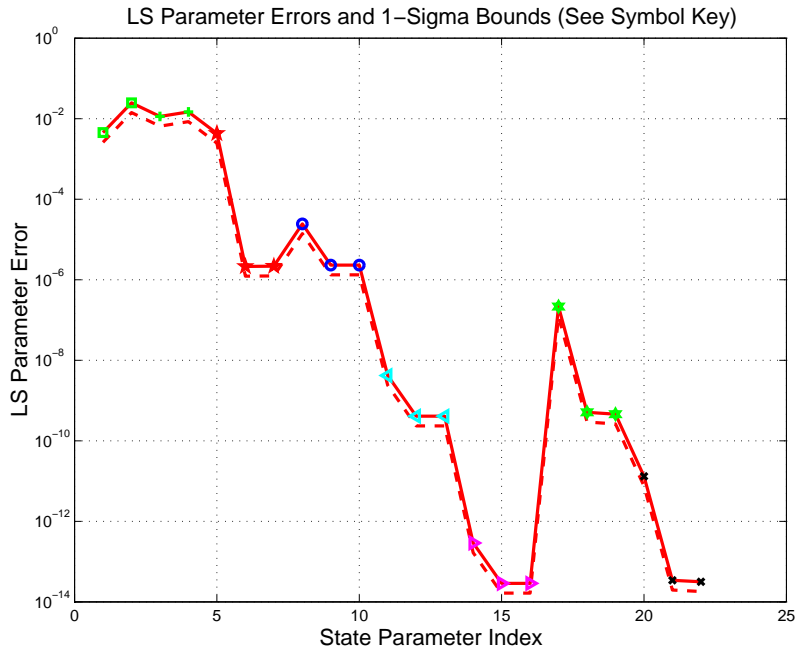


Figure 3.14: LS parameter error sigma plot

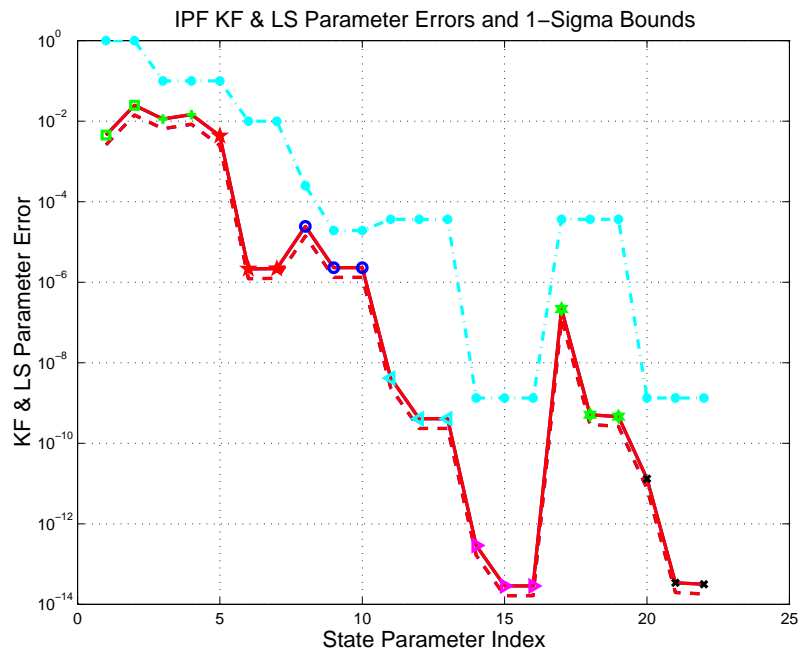


Figure 3.15: KF and LS parameter error sigma plot

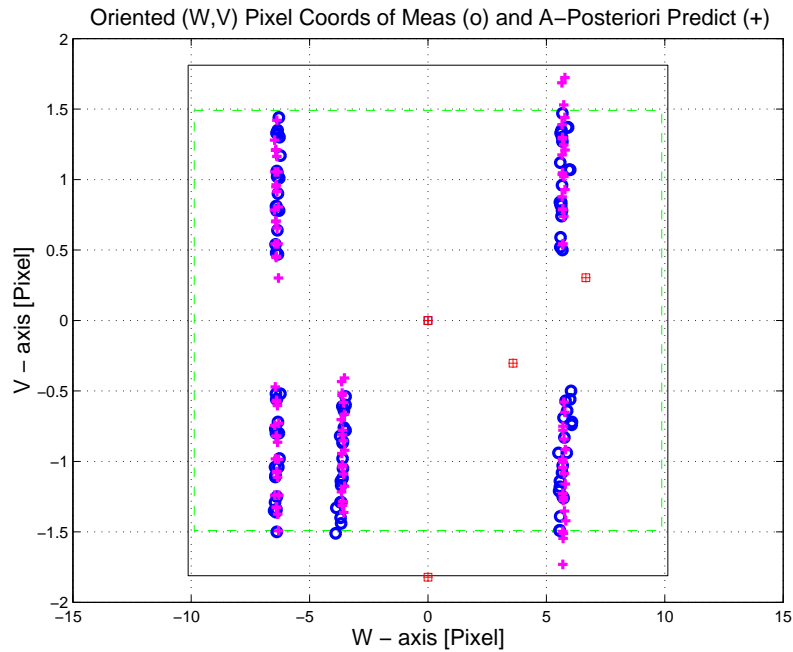


Figure 3.16: Oriented Pixel Coords of meas. and a-posteriori predicts

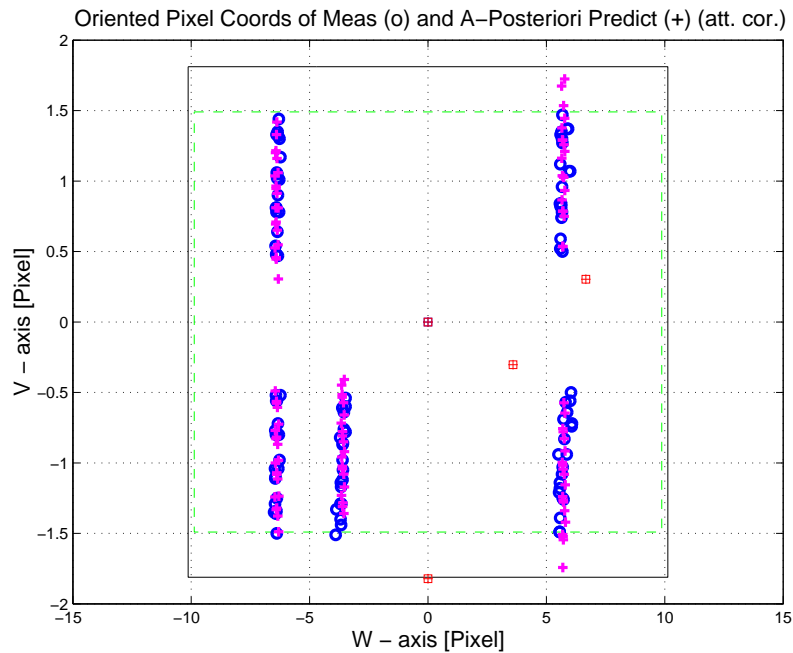


Figure 3.17: Oriented Pixel Coords of meas. and a-posteriori predicts (attitude corrected)

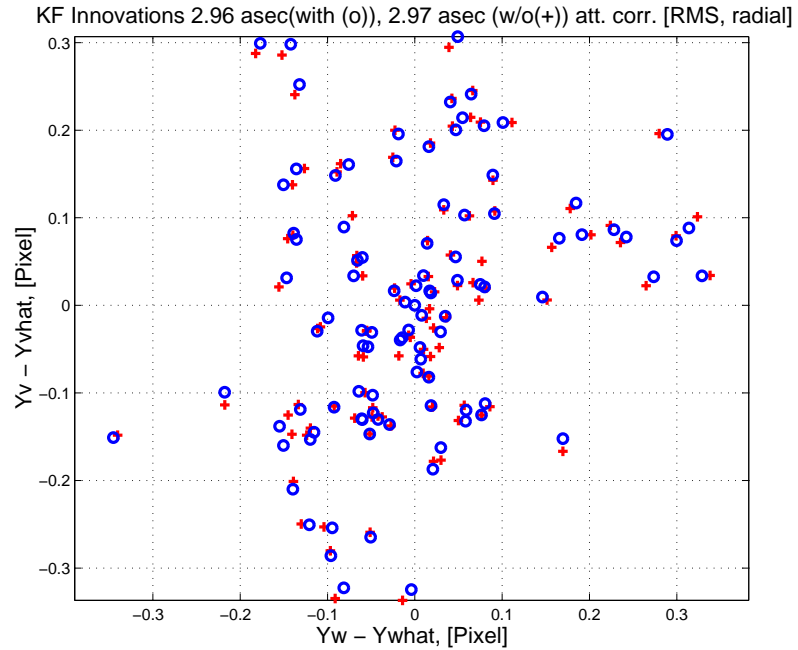


Figure 3.18: KF innovations with (o) and w/o (+) attitude corrections

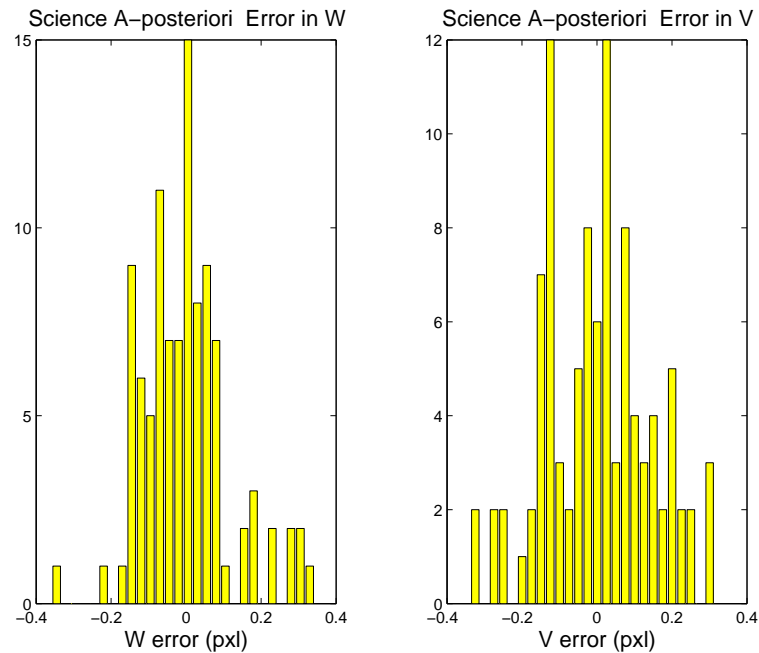


Figure 3.19: Histograms of science a-posteriori residuals (or innovations)

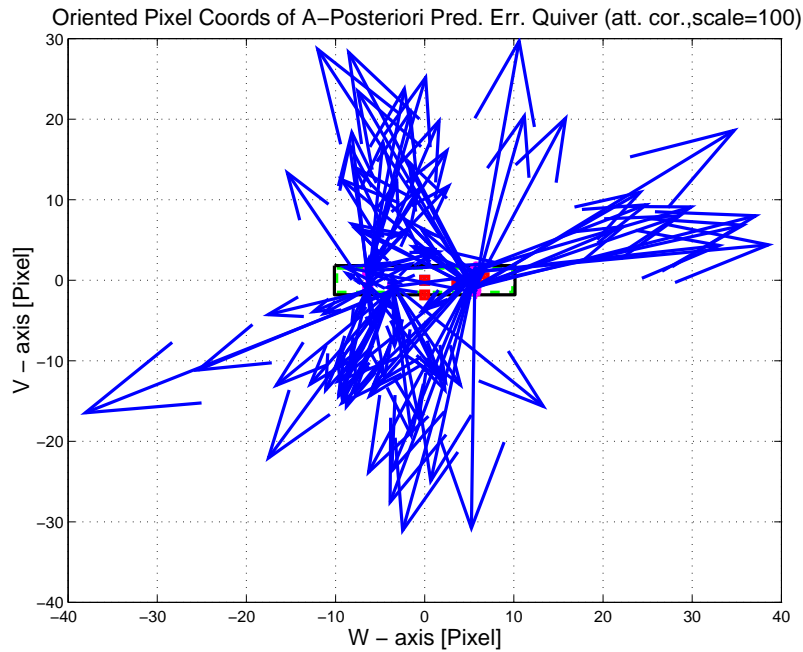


Figure 3.20: A-Posteriori Science Centroid Prediction Error Quiver (Att. Cor.)

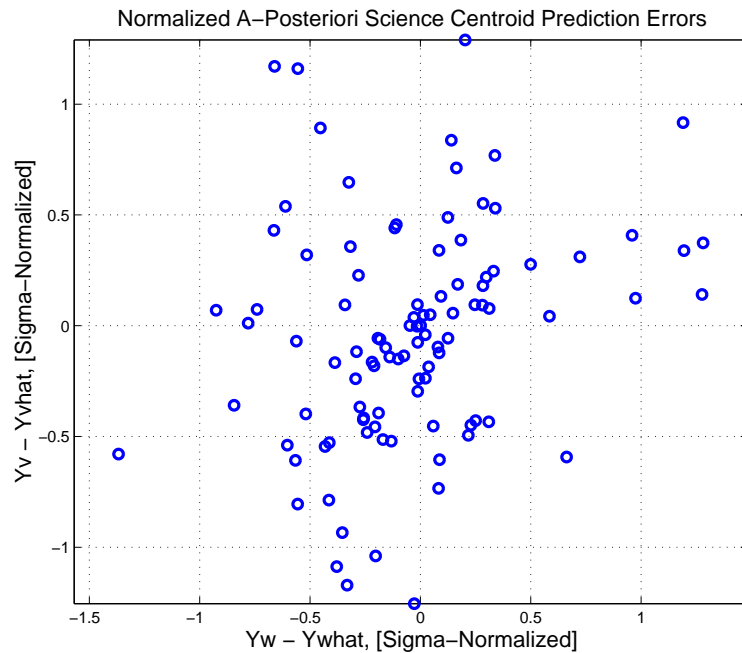


Figure 3.21: Normalized A-Posteriori Science Centroid Prediction Errors

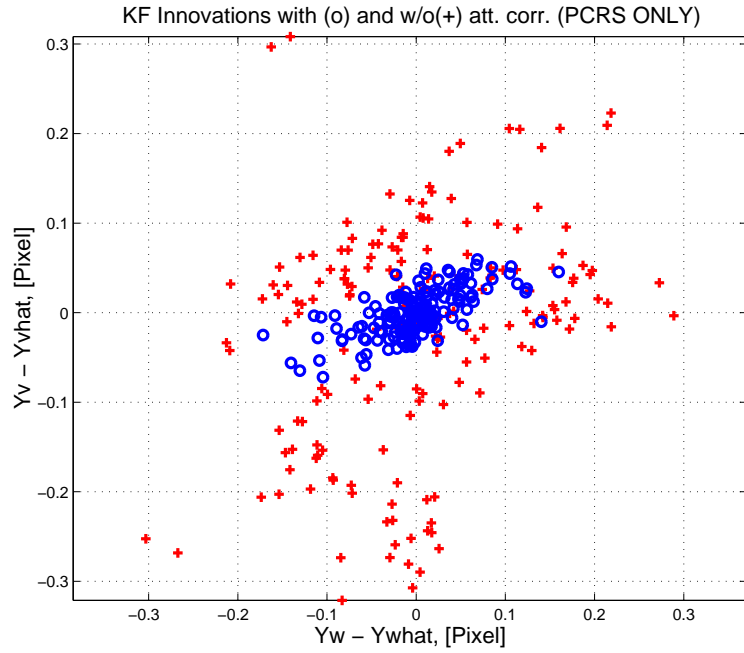


Figure 3.22: KF innovations with (o) and w/o (+) attitude corrections (PCRS)

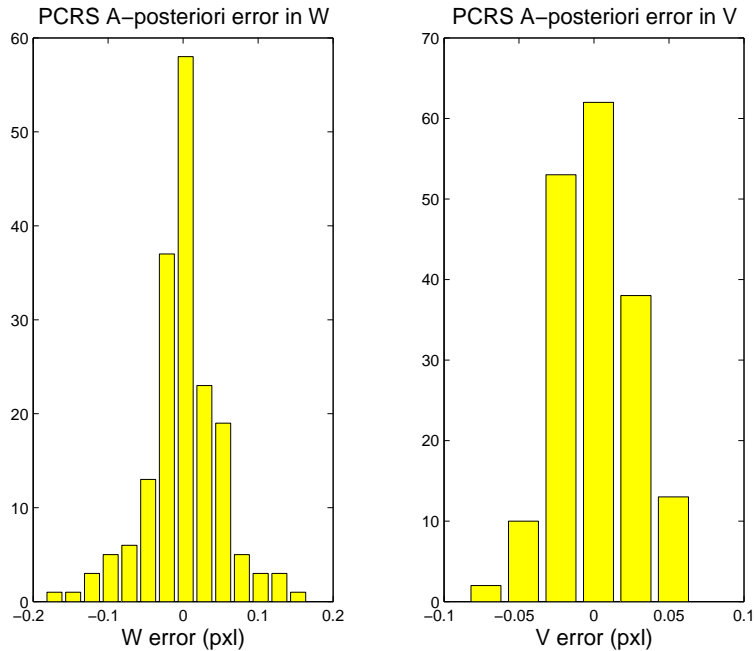


Figure 3.23: Histograms of PCRS a-posteriori residuals (or innovations)

IPF PCRS SUMMARY						
PCRS 1 (Total of 118 centroids)						
RMS	MEAN		SIGMA			
METRIC	APOST.	ATT. COR.	APOST.	ATT. COR.	STAT. CONF.	UNITS
Radial	0.0167	0.0040	0.1689	0.0651	0.0060	arcsec
W-axis	0.0014	-0.0000	0.1165	0.0588	0.0054	arcsec
V-axis	-0.0166	0.0040	0.1223	0.0280	0.0026	arcsec
PCRS 2 (Total of 60 centroids)						
METRIC	APOST.	ATT. COR.	APOST.	ATT. COR.	STAT. CONF.	UNITS
Radial	0.0205	0.0087	0.1604	0.0268	0.0035	arcsec
W-axis	-0.0043	0.0000	0.0970	0.0214	0.0028	arcsec
V-axis	-0.0200	-0.0087	0.1278	0.0162	0.0021	arcsec
Combined (Total of 178 centroids)						
METRIC	APOST.	ATT. COR.	APOST.	ATT. COR.	STAT. CONF.	UNITS
Radial	0.0178	0.0003	0.1661	0.0555	0.0042	arcsec
W-axis	-0.0005	-0.0000	0.1103	0.0494	0.0037	arcsec
V-axis	-0.0178	-0.0003	0.1242	0.0254	0.0019	arcsec

Table 3.3: PCRS measurement prediction error summary

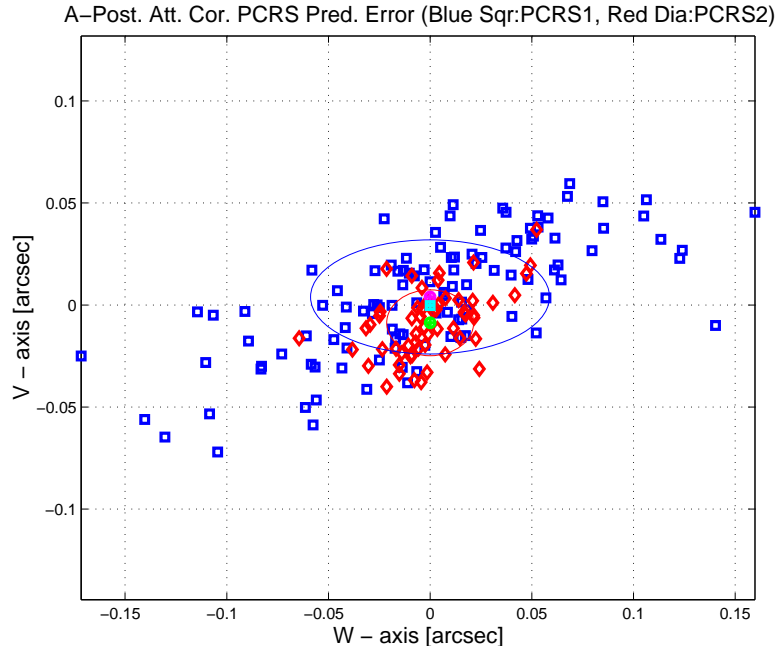


Figure 3.24: A-posteriori PCRS Prediction Summary

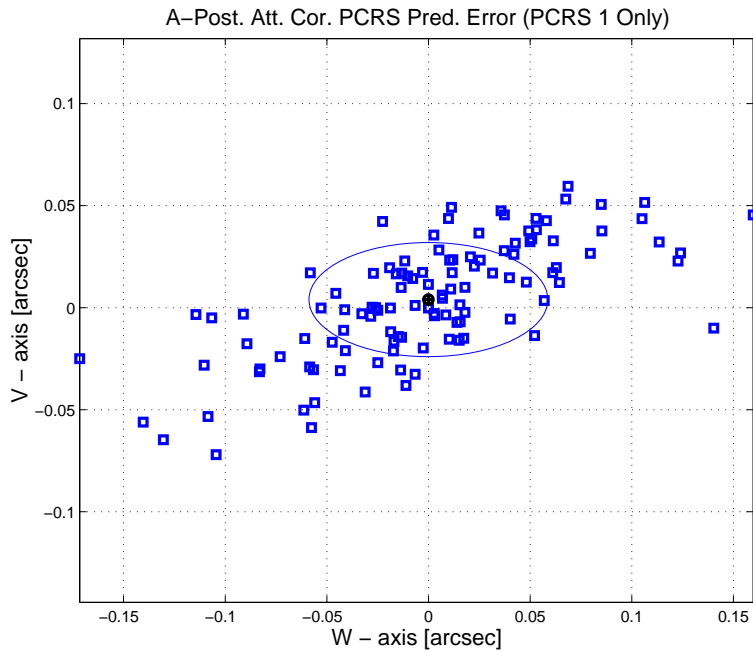


Figure 3.25: A-posteriori PCRS Prediction (PCRS 1 Only)

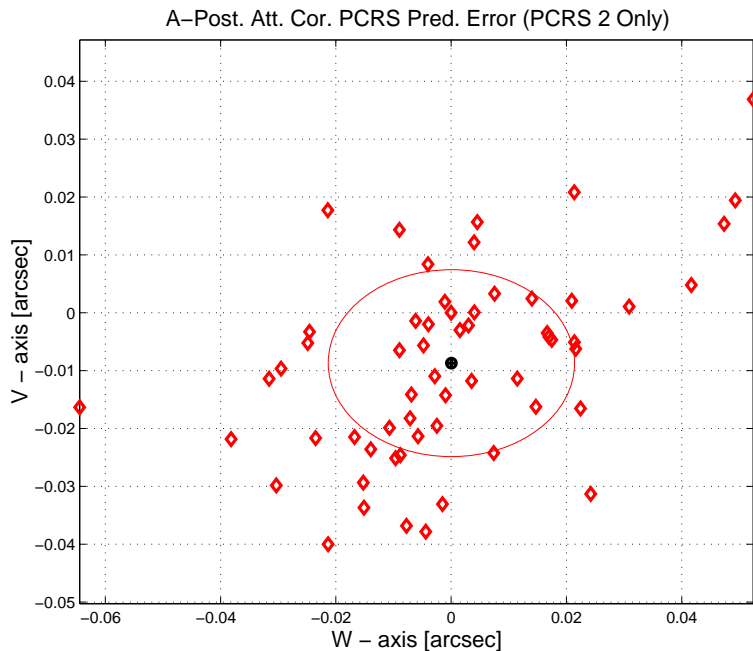


Figure 3.26: A-posteriori PCRS Prediction (PCRS 2 Only)

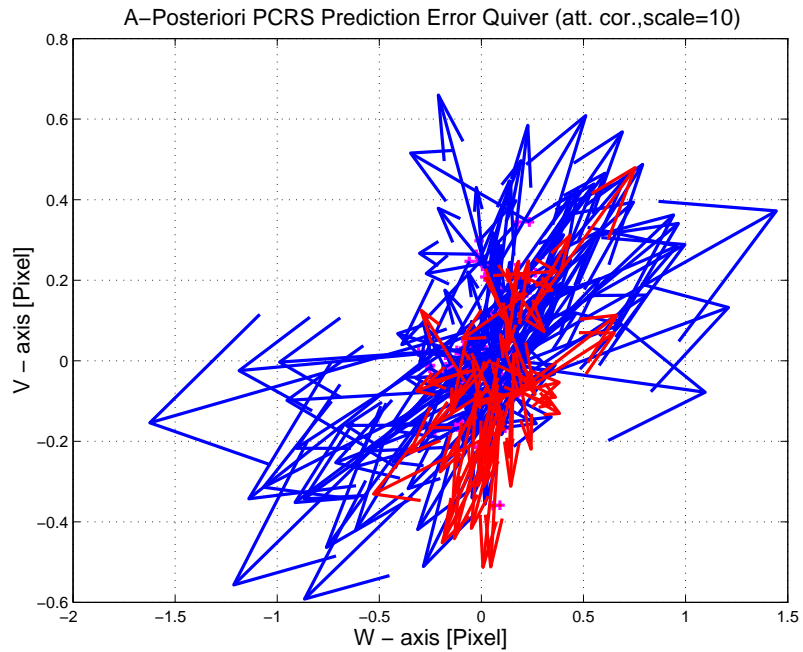


Figure 3.27: A–Posteriori PCRS Prediction Errors Quiver (Att. Cor.)

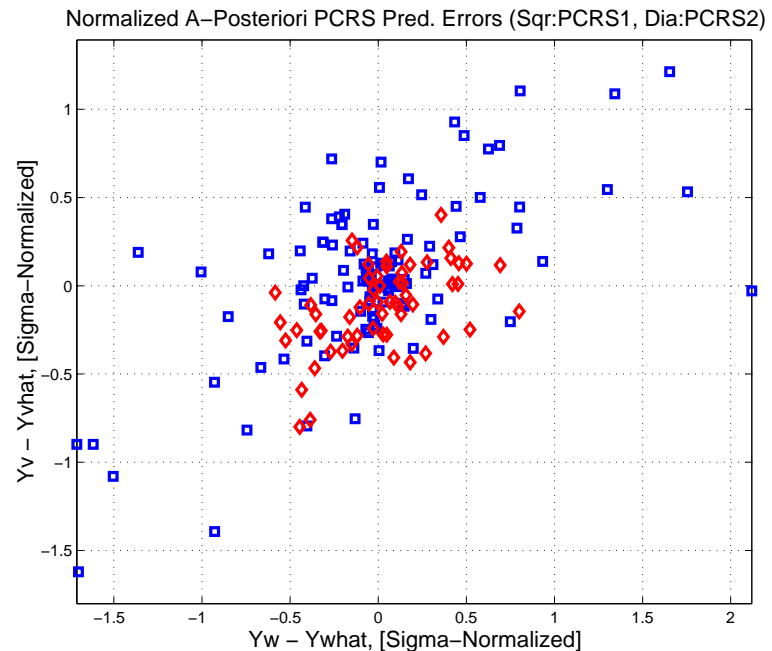


Figure 3.28: Normalized A–Posteriori PCRS Prediction Errors

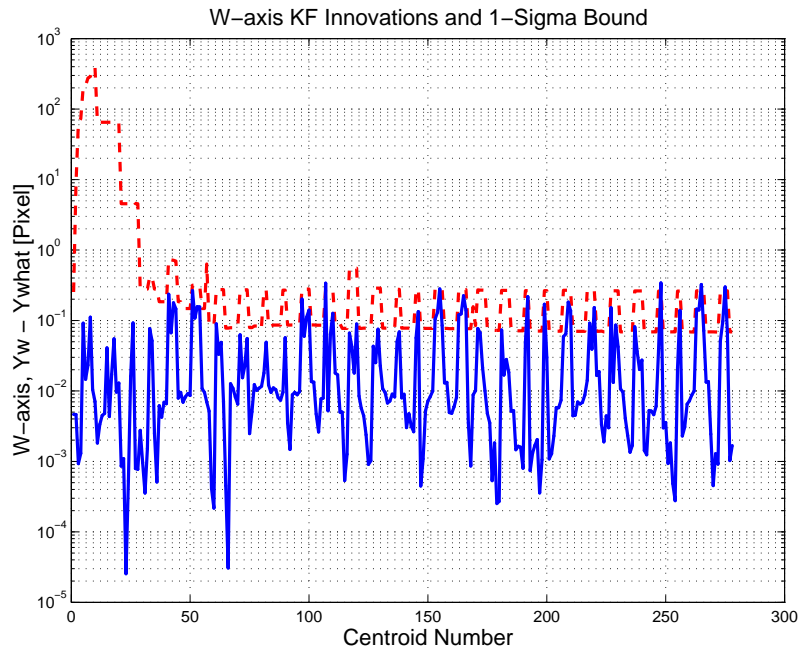


Figure 3.29: W-axis KF innovations and 1-sigma bound

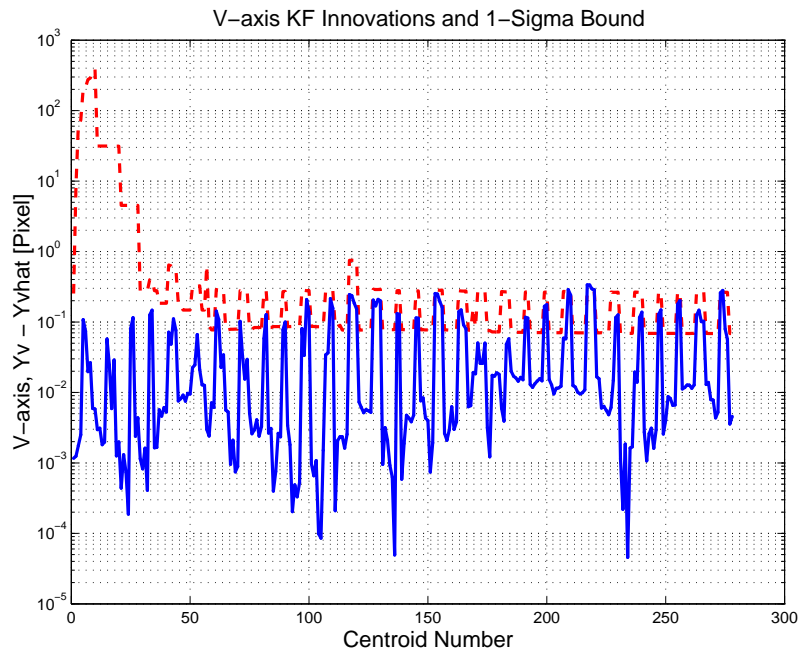


Figure 3.30: V-axis KF innovations and 1-sigma bound

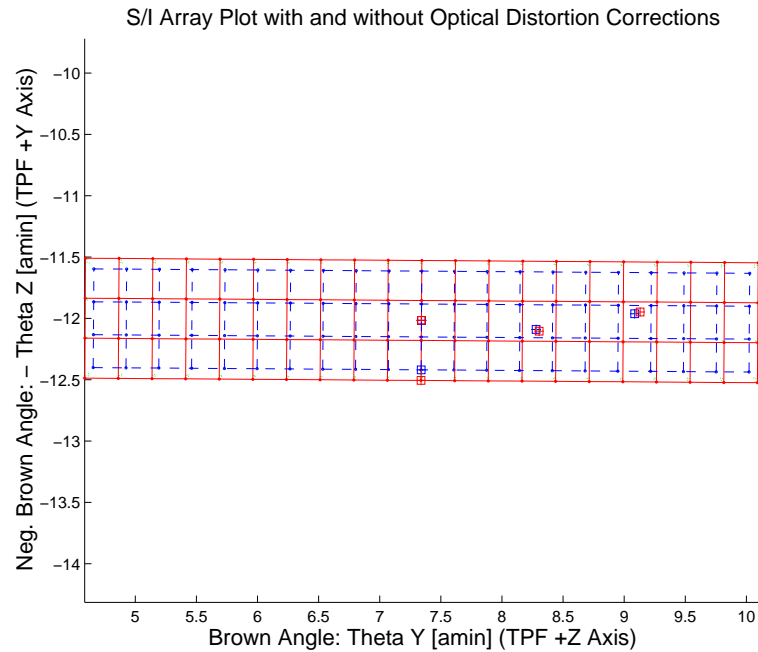


Figure 3.31: Array plot with (solid) and w/o (dashed) optical distortion corrections

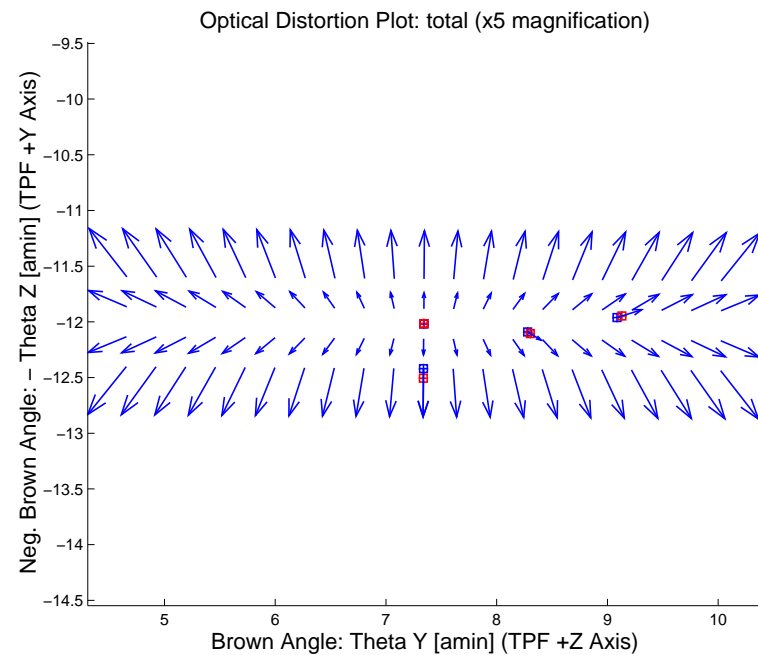


Figure 3.32: Optical Distortion Plot: total (x5 magnification)

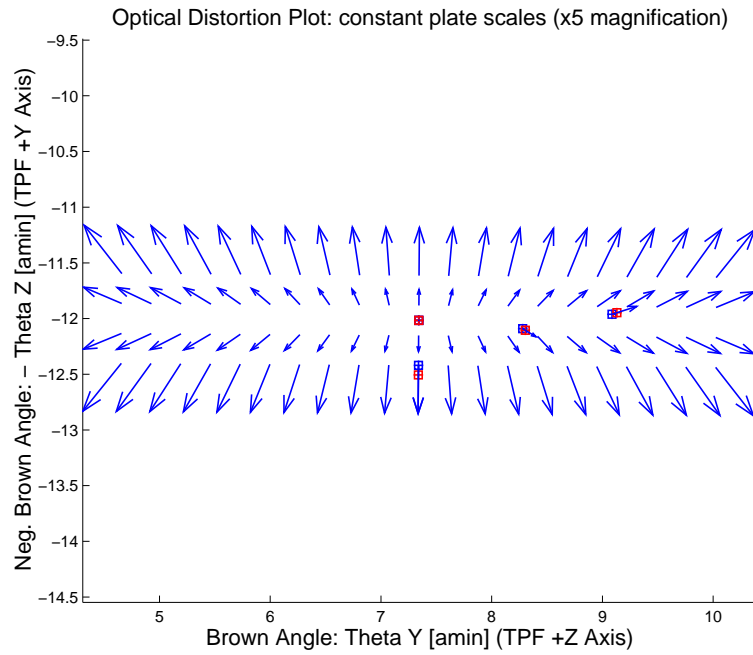


Figure 3.33: Optical Distortion Plot: constant plate scales (x5 magnification)

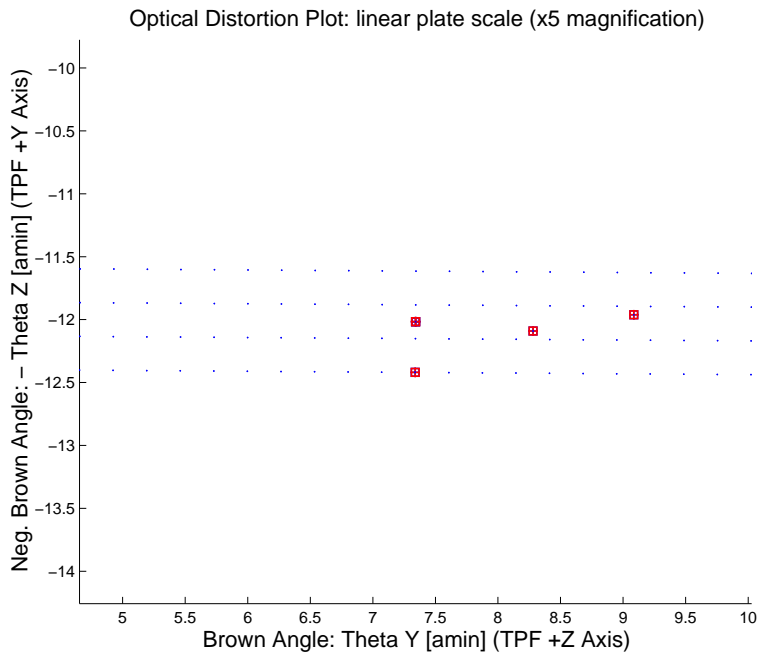


Figure 3.34: Optical Distortion Plot: linear plate scale (x5 magnification)

Opt. Dist. Plot: Γ depdt; $\Gamma = -3.95468e-004$ in blue and $\Gamma = 1.97734e-004$ in red (x5 magn)

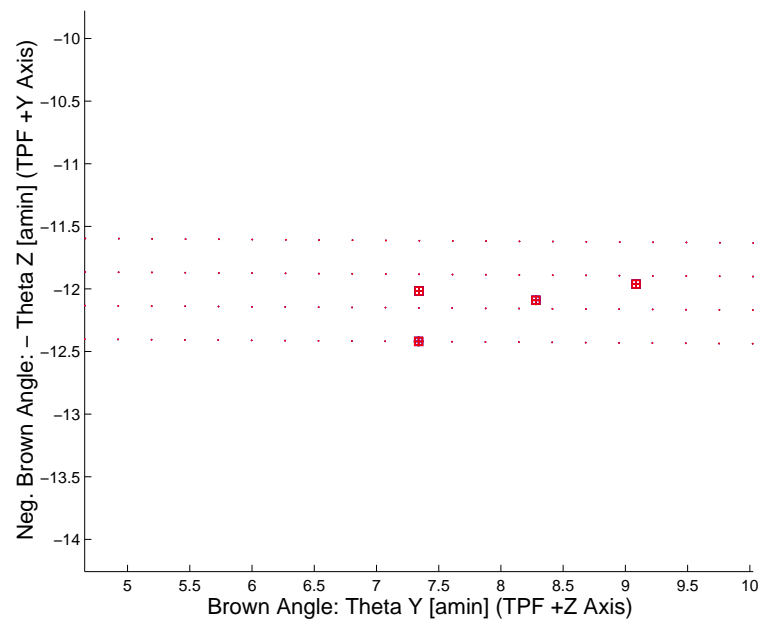


Figure 3.35: Optical Distortion Plot: gamma terms (x5 magnification)

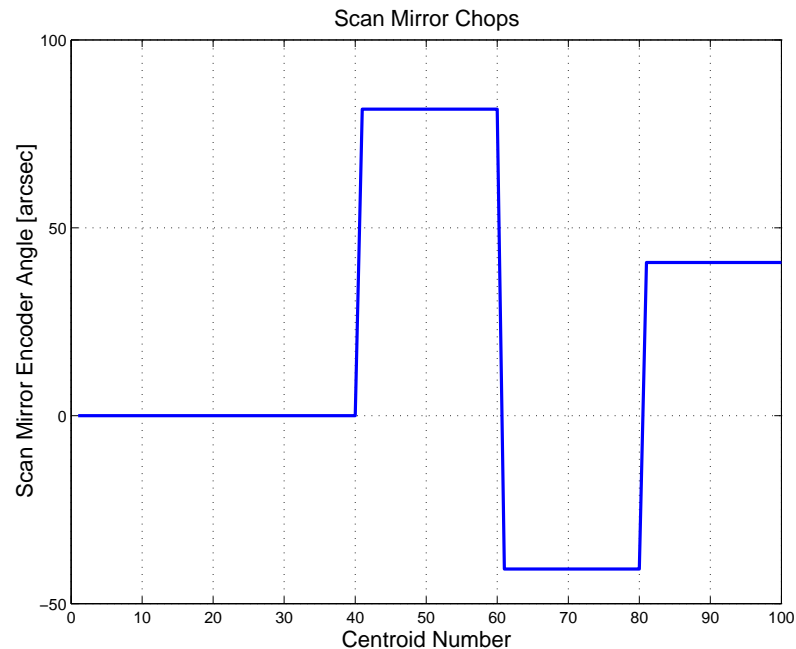


Figure 3.36: Scan Mirror Chops

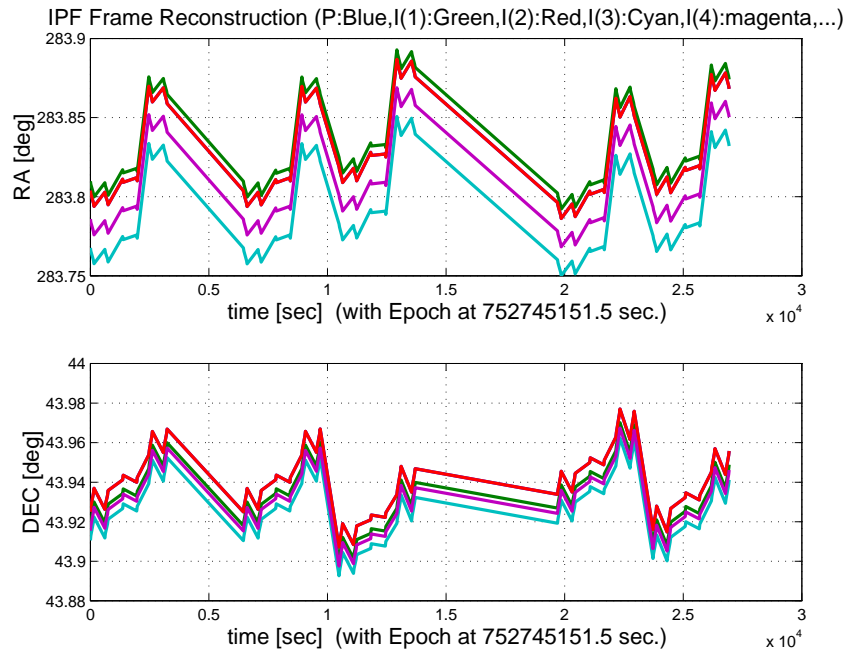


Figure 3.37: IPF Frame Reconstruction

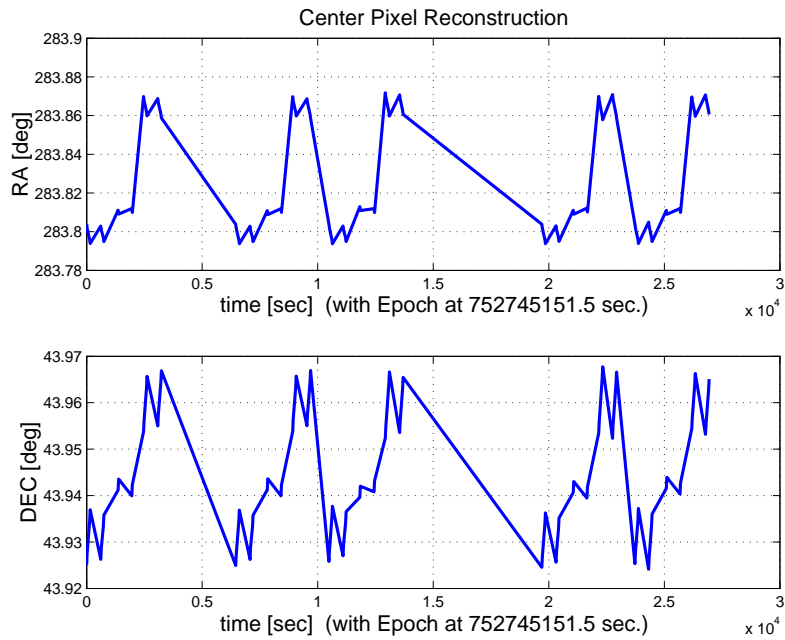


Figure 3.38: Center Pixel Reconstruction

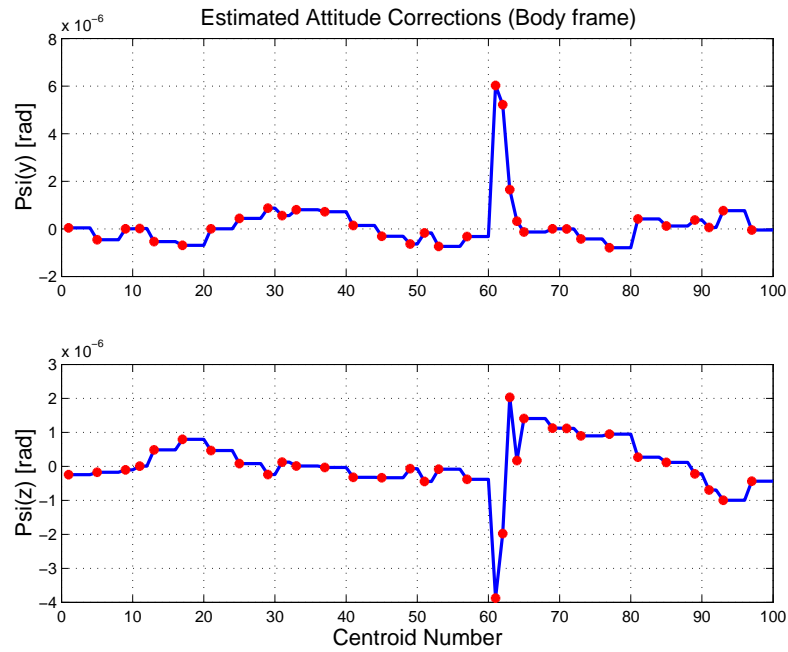


Figure 3.39: Estimated attitude corrections (Body frame)

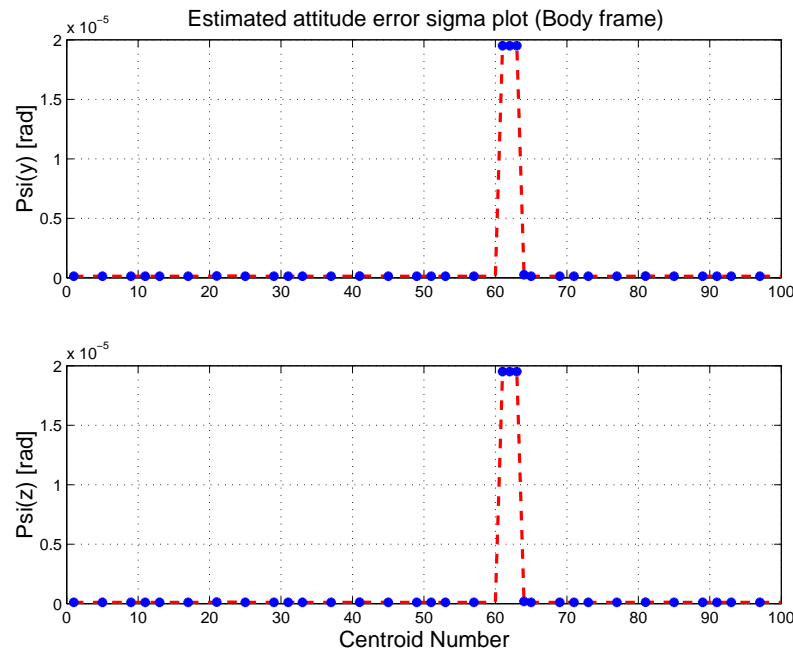


Figure 3.40: Estimated attitude error sigma plot (Body frame)

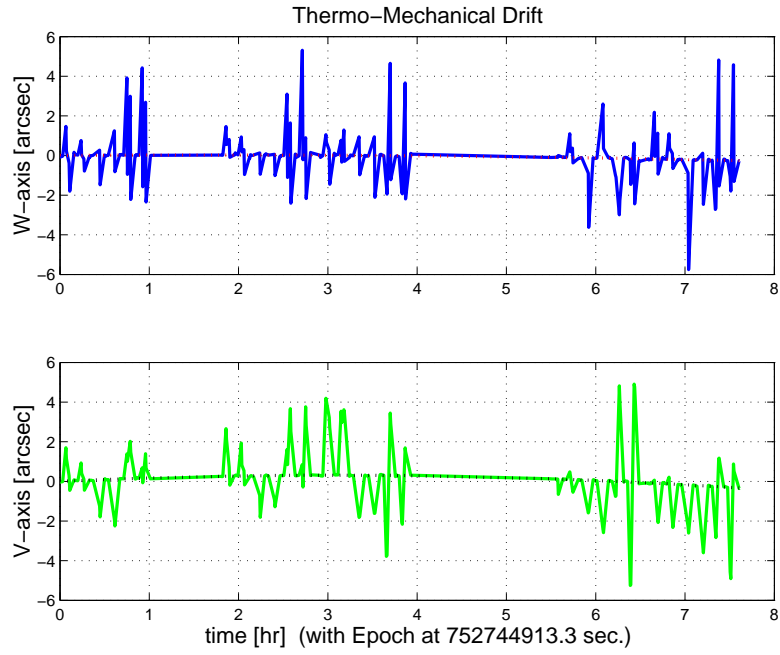


Figure 3.41: Thermo-mechanical boresight drift (equiv. angle in (W,V) coords)

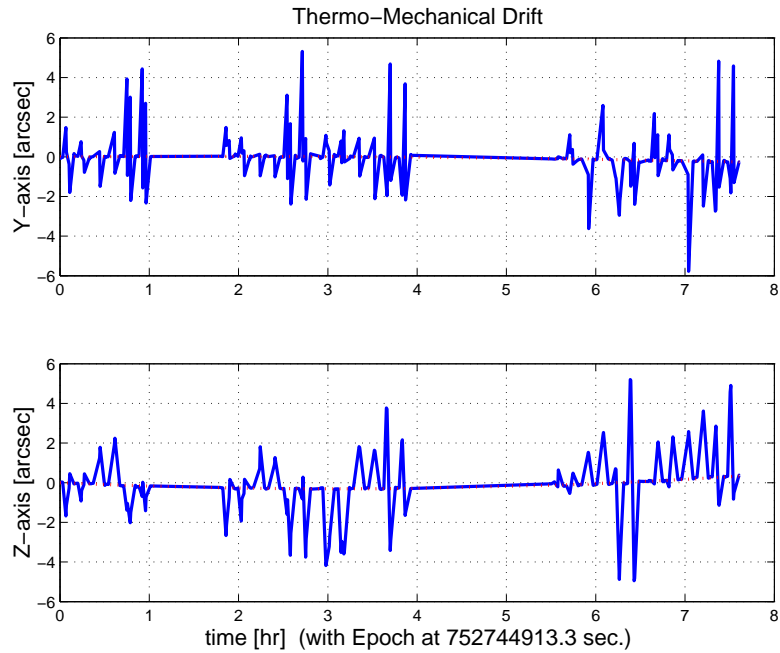


Figure 3.42: Thermo-mechanical boresight drift (equiv. angle in Body frame)

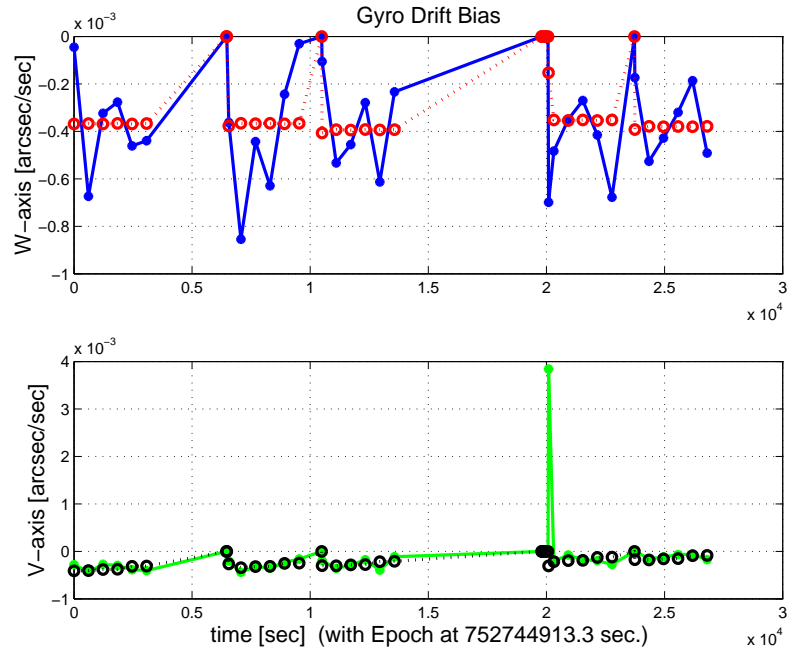


Figure 3.43: Gyro drift bias contribution (equiv. rate in (W,V) coords)

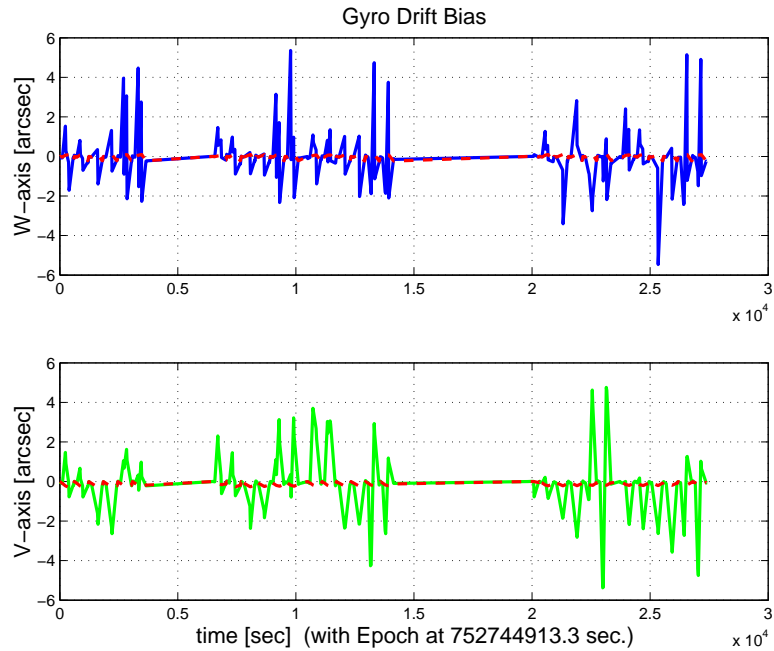


Figure 3.44: Gyro drift bias contribution (equiv. angle in (W,V) coords)

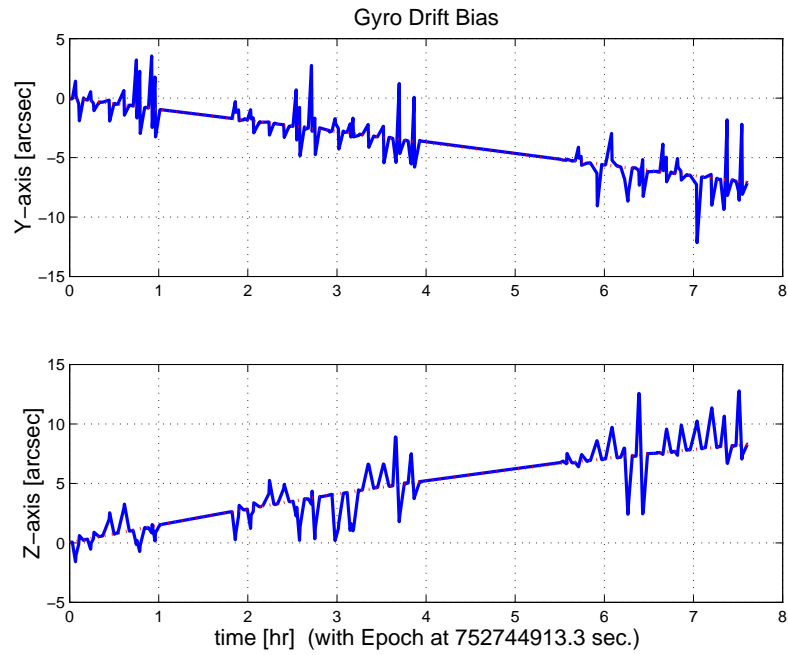


Figure 3.45: Gyro drift bias contribution (equiv. angle in Body frame)

3.2 IPF OUTPUT DATA (IF MINI FILE)

```

OUTPUT FILE NAME: IFmini504087.dat    DATE: 04-Dec-2003    TIME: 16:03
INSTRUMENT NAME: MIPS_160um_center_large_FOV   NF: 87
IPF FILTER VERSION: IPF.V3.0.0B      SW RELEASE DATE: November 3, 2003
FRAME TABLE USED: BodyFrames_FTU_14a
-----
----- IPF BROWN ANGLE SUMMARY -----
----- WAS -----      ----- IS -----
Frame  theta_Y     theta_Z     angle      theta_Y     theta_Z     angle
Number (arcmin) (arcmin) (deg)      (arcmin) (arcmin) (deg)
----- -----
087    +7.347515  +12.105588  +0.000006  +7.341460  +12.017026  +0.384662
088    +7.347515  +12.554659  +0.000006  +7.338177  +12.505950  +0.384662
089    +7.347515  +12.105588  +0.000006  +7.341460  +12.017026  +0.384662
091    +9.077043  +12.030743  +0.000006  +9.130996  +11.947549  +0.384662
092    +8.278799  +12.180433  +0.000006  +8.304215  +12.104981  +0.384662
-----
OFFSET      NF      Delta_CW      Delta_CV
  0        87      +0.000      +0.000      pixels
OFFSET FRAME NAME: MIPS_160um_center_large_FOV
Brown Angle  theta_Y(arcmin)  theta_Z(arcmin)  angle(deg)
WAS(FTB)      +7.347515      +12.105588      +0.000006
IS (EST)      +7.341460      +12.017026      +0.384662
dT_EST       -0.006055      -0.088562      +0.384656
T_ssSIGMA    +0.004213      +0.004257      +0.140969
dT_EST/T_ssSIGMA -1.437309      -20.801432      +2.728659
-----
OFFSET      NF      Delta_CW      Delta_CV
  1        88      +0.000      -1.500      pixels
OFFSET FRAME NAME: MIPS_160um_plusY_edge
Brown Angle  theta_Y(arcmin)  theta_Z(arcmin)  angle(deg)
WAS(FTB)      +7.347515      +12.554659      +0.000006
IS (EST)      +7.338177      +12.505950      +0.384662
dT_EST       -0.009337      -0.048708      +0.384656
T_ssSIGMA    +0.004342      +0.006515      +0.140969
dT_EST/T_ssSIGMA -2.150735      -7.476843      +2.728659
-----
OFFSET      NF      Delta_CW      Delta_CV
  2        89      +0.000      +0.000      pixels
OFFSET FRAME NAME: MIPS_160um_large_only
Brown Angle  theta_Y(arcmin)  theta_Z(arcmin)  angle(deg)
WAS(FTB)      +7.347515      +12.105588      +0.000006
IS (EST)      +7.341460      +12.017026      +0.384662
dT_EST       -0.006055      -0.088562      +0.384656
T_ssSIGMA    +0.004213      +0.004257      +0.140969
dT_EST/T_ssSIGMA -1.437309      -20.801432      +2.728659
-----
OFFSET      NF      Delta_CW      Delta_CV
  3        91      +6.500      +0.250      pixels
OFFSET FRAME NAME: MIPS_160um_small_FOV1
Brown Angle  theta_Y(arcmin)  theta_Z(arcmin)  angle(deg)
WAS(FTB)      +9.077043      +12.030743      +0.000006
IS (EST)      +9.130996      +11.947549      +0.384662
dT_EST       +0.053954      -0.083194      +0.384656
T_ssSIGMA    +0.006648      +0.006645      +0.140969
dT_EST/T_ssSIGMA +8.115465      -12.519774      +2.728659
-----
OFFSET      NF      Delta_CW      Delta_CV
  4        92      +3.500      -0.250      pixels
OFFSET FRAME NAME: MIPS_160um_small_FOV2

```

Brown Angle	theta_Y(arcmin)	theta_Z(arcmin)	angle(deg)	
WAS(FTB)	+8.278799	+12.180433	+0.000006	
IS (EST)	+8.304215	+12.104981	+0.384662	
dT_EST	+0.025416	-0.075452	+0.384656	
T_ssSIGMA	+0.005189	+0.005156	+0.140969	
dT_EST/T_ssSIGMA	+4.897548	-14.634124	+2.728659	
-----	-----	-----	-----	
-----	-----	-----	-----	
VARNAME	MEAN	SIGMA	SCALED_SIGMA	
a00	+2.5721927514763883E-002	+4.4998584814644480E-003	+2.5792583712716420E-003	
b00	+2.1474433140533347E-001	+2.4674550887208491E-002	+1.4143120765986568E-002	
del_alpha	+6.2528107691584012E-015	+1.1231892262385775E-002	+6.4379696077801135E-003	
beta	+9.5171248469256298E-001	+1.4508581297081297E-002	+8.3161237003154774E-003	
del_theta1	+3.0104391202101510E-014	+4.2924436284496196E-003	+2.4603709666636488E-003	
del_theta2	-5.5642269284514833E-017	+2.1379385677017178E-006	+1.2254376378109051E-006	
del_theta3	-3.3153081313770129E-017	+2.1606490083021940E-006	+1.2384549568174759E-006	
del_arx	+9.1610730884467422E-015	+2.4224273420360518E-005	+1.3885027776941131E-005	
del_ary	-4.3611410348408776E-018	+2.2862272185529796E-006	+1.3104346984180691E-006	
del_arz	-2.2659249687240706E-017	+2.2865879811362036E-006	+1.3106414654839455E-006	
brx	+1.4191154083040012E-009	+4.1545168899557804E-009	+2.3813132148814963E-009	
bry	+3.6296643523468391E-011	+4.0488896451358717E-010	+2.3207690985368765E-010	
brz	-2.6712518926380224E-010	+4.0492093304185676E-010	+2.3209523378420596E-010	
crx	-9.4306528250449969E-014	+2.8979374195264281E-013	+1.6610587598528977E-013	
cry	-5.9926268042183496E-015	+2.8587770069196839E-014	+1.6386125379429310E-014	
crz	+2.3781296692493194E-014	+2.8588526630812220E-014	+1.6386559030373645E-014	
bgx	+5.8782690934854781E-007	+2.1480373692392482E-007	+1.2312261350520471E-007	
bgy	-1.2699354388006659E-009	+5.0858346028291409E-010	+2.9151320043249422E-010	
bgz	+2.0908383213876221E-009	+4.5627146425790084E-010	+2.6152866775858367E-010	
cgx	+4.0139153277639364E-013	+1.3089075355611346E-011	+7.5024819829842547E-012	
cgy	+9.8126112470758217E-016	+3.4261879898216281E-014	+1.9638448832777168E-014	
cgz	-4.6117151231918434E-014	+3.1502590991522584E-014	+1.8056861536051664E-014	
-----	-----	-----	-----	
LSQF RESIDUAL SIGMA SCALE =	+5.7318655284293296E-001			
-----	-----	-----	-----	
-----	-----	-----	-----	
	a_mirror(1)	a_mirror(2)	a_mirror(3)	
a_mirror_ipf	+0.0000000000000000E+000	+2.5377820298621276E-002	+9.9967793125430704E-001	
a_mirror_tpf	-2.0699089529566117E-003	+1.8673187304126954E-002	+9.9982349819997307E-001	
beta	beta_0	beta	beta_total	
	+2.8047410000000001E-006	+9.5171248469256298E-001	+2.6693070260291039E-006	
-----	-----	-----	-----	
qT	qT(1)	qT(2)	qT(3)	qT(4)
FrmTbl:	-1.8265322546296800E-006	-1.0686509308528700E-003	-1.7606843785389101E-003	+9.9999787898393599E-001
Estim:	+3.3549321122310809E-003	-1.0736312146621037E-003	-1.7442095038269984E-003	+9.9999227471003194E-001
DelTheta	deltheta(1)	deltheta(2)	deltheta(3)	
	+6.7135684095382129E-003	+1.7613343438303747E-006	+2.5761577677907642E-005	[rad]
EulAngT	theta(1)	theta(2)	theta(3)	[rad]
Mean	+6.7136234065858242E-003	-2.1355440553579123E-003	-3.4956110681961228E-003	
SigmaT	+4.2924436284496196E-003	+2.1379385677017178E-006	+2.1606490083021940E-006	
-----	-----	-----	-----	
qR	qR(1)	qR(2)	qR(3)	qR(4)
ASFILe:	+7.1086635580286384E-004	+1.2695571640506387E-003	-1.6159859660547227E-004	+9.9999892711639404E-001
Estim:	+6.7963618456269061E-004	+1.2700538258751716E-003	-1.6037061983579197E-004	+9.9999894966904856E-001
DelThetaR	delthetaR(1)	delthetaR(2)	delthetaR(3)	
	-6.2463584944210326E-005	+9.8499187674153929E-007	+2.3759243388572227E-006	[rad]
EulAngR	angR(1)	angR(2)	angR(3)	[rad]
Mean	+1.3588683855561376E-003	+2.5403257033762595E-003	-3.1901558846925327E-004	
SigmaR	+2.4224273420360518E-005	+2.2862272185529796E-006	+2.2865879511362036E-006	
-----	-----	-----	-----	
Initial Gyro Bias	Bg0(1)	Bg0(2)	Bg0(3)	
	-4.1339711742693908E-007	-2.0063052375007828E-007	+3.6787506019209104E-007	
Gyro Bias Correction	Bg(1)	Bg(2)	Bg(3)	

```

+5.8782690934854781E-007 -1.2699354388006659E-009 +2.0908383213876221E-009
Total Gyro Bias      BgT(1)          BgT(2)          BgT(3)
+1.7442979192160874E-007 -2.0190045918887895E-007 +3.6996589851347864E-007

Initial Gyro Bias Rate   Cg0(1)          Cg0(2)          Cg0(3)
+0.0000000000000000E+000 +0.0000000000000000E+000 +0.0000000000000000E+000
Gyro Bias Rate Correction Cg(1)           Cg(2)           Cg(3)
+4.0139153277639364E-013 +9.8126112470758217E-016 -4.6117151231918434E-014
Total Gyro Bias Rate     CgT(1)          CgT(2)          CgT(3)
+4.0139153277639364E-013 +9.8126112470758217E-016 -4.6117151231918434E-014
-----

```

OFFSET	NF	Delta_CW	Delta_CV
1	88	+0.000	-1.500 pixels

OFFSET FRAME NAME: MIPS_160um_plusY_edge

qT	qT(1)	qT(2)	qT(3)	qT(4)
----	-------	-------	-------	-------

WAS(FTB)	-1.8963308941670110E-006	-1.0686507929678407E-003	-1.8259989907623111E-003	+9.9999776185228151E-001
IS (EST)	+3.3548566266421442E-003	-1.0733923582066944E-003	-1.8153217668055465E-003	+9.9999214865554975E-001

DelTheta	deltheta(1)	deltheta(2)	deltheta(3)
Units	rad	rad	rad

EulAngT	theta(1)	theta(2)	theta(3)	[rad]
---------	----------	----------	----------	-------

Mean	+6.7136234065858233E-003	-2.1345891937813413E-003	-3.6378334946712328E-003
sSigmaT	+2.4603709477200612E-003	+1.2628990299221808E-006	+1.8950135864315476E-006
SigmaT	+4.2924435954000174E-003	+2.2032949371515451E-006	+3.3061026589554821E-006

OFFSET	NF	Delta_CW	Delta_CV
2	89	+0.000	+0.000 pixels

OFFSET FRAME NAME: MIPS_160um_large_only

qT	qT(1)	qT(2)	qT(3)	qT(4)
----	-------	-------	-------	-------

WAS(FTB)	-1.8265322546296804E-006	-1.0686509308528702E-003	-1.7606843785389105E-003	+9.9999787898393622E-001
IS (EST)	+3.3549321122310809E-003	-1.0736312146621034E-003	-1.7442095038269984E-003	+9.9999227471003194E-001

DelTheta	deltheta(1)	deltheta(2)	deltheta(3)
Units	rad	rad	rad

EulAngT	theta(1)	theta(2)	theta(3)	[rad]
---------	----------	----------	----------	-------

Mean	+6.7136234065858242E-003	-2.1355440553579119E-003	-3.4956110681961224E-003
sSigmaT	+2.4603709666636488E-003	+1.2254376378109051E-006	+1.2384549568174757E-006
SigmaT	+4.2924436284496196E-003	+2.1379385677017178E-006	+2.1606490080321936E-006

OFFSET	NF	Delta_CW	Delta_CV
3	91	+6.500	+0.250 pixels

OFFSET FRAME NAME: MIPS_160um_small_FOV1

qT	qT(1)	qT(2)	qT(3)	qT(4)
----	-------	-------	-------	-------

WAS(FTB)	-2.2550603563025619E-006	-1.3202000341957709E-003	-1.7497980854334510E-003	+9.9999759763383667E-001
IS (EST)	+3.3544896331269003E-003	-1.3338728130085705E-003	-1.7332303622965533E-003	+9.9999198201542150E-001

DelTheta	deltheta(1)	deltheta(2)	deltheta(3)
Units	rad	rad	rad

EulAngT	theta(1)	theta(2)	theta(3)	[rad]
---------	----------	----------	----------	-------

Mean	+6.7136234065858233E-003	-2.6560991525776041E-003	-3.475401110350973E-003
sSigmaT	+2.4603705414310505E-003	+1.9338962093967430E-006	+1.9329454825980906E-006
SigmaT	+4.2924428865749259E-003	+3.3739385542191485E-006	+3.3722798851629103E-006

OFFSET	NF	Delta_CW	Delta_CV
4	92	+3.500	-0.250 pixels

OFFSET FRAME NAME: MIPS_160um_small_FOV2

qT	qT(1)	qT(2)	qT(3)	qT(4)
----	-------	-------	-------	-------

```

WAS(FTB) -2.0781242430031014E-006 -1.2041004277977808E-003 -1.7715698889046410E-003 +9.9999770583635350E-001
IS (EST) +3.3546713130422467E-003 -1.2137000775779545E-003 -1.7565315978239284E-003 +9.9999209382337073E-001

DelTheta      deltheta(1)          deltheta(2)          deltheta(3)
Units         rad               rad               rad
              +6.7135662048870169E-003 -7.3931171731866818E-006 +2.1948168861156229E-005
EulAngT       theta(1)          theta(2)          theta(3)          [rad]
Mean          +6.7136234065858233E-003 -2.4155981405927420E-003 -3.5211961001230209E-003
sSigmaT        +2.4603708216945630E-003 +1.5095553390527081E-006 +1.4997981672865333E-006
SigmaT         +4.2924433755318131E-003 +2.6336195983061781E-006 +2.6165969174393986E-006
-----
----- q(1)           q(2)           q(3)           q(4)
PCRS1A: +5.3371888965461637E-007 +3.7444233778550031E-004 -1.4253684912431913E-003 +9.9999891405806784E-001
PCRS2A: -5.2779261998836216E-007 +3.8462959425181312E-004 +1.3722087221825403E-003 +9.9999898455099423E-001
-----
***** CS-FILE PARAMETERS: ***** AS-FILE PARAMETERS: *****
Row (01) PIX2RADX: +7.805500299999999E-005 Row (1) TASTART: +7.5274400029071045E+008
Row (02) PIX2RADY: +7.805500299999999E-005 Row (2) TASTOP: +7.5277300039073789E+008
Row (03) CXO: +1.0500000000000000E+001 Row (3) S/C TIME: +7.5271691689080811E+008
Row (04) CYO: +2.0000000000000000E+000 Row (4) QR1: +7.1086635580286384E-004
Row (05) BETA0: +2.8047410000000001E-006 Row (5) QR2: +1.2695571640506387E-003
Row (06) GAMMA_E0: +2.0070000000000000E+003 Row (6) QR3: -1.6159859660547227E-004
Row (07) D11: -1.0000000000000000E+000 Row (7) QR4: +9.9999892711639404E-001
Row (08) D12: +0.0000000000000000E+000
Row (09) D21: +0.0000000000000000E+000
Row (10) D22: -1.0000000000000000E+000
Row (11) DG: -1.0000000000000000E+000
-----
----- INITIAL STA-TO-PCRS ALIGNMENT (R) KNOWLEDGE (1-SIGMA)
SIGMA(X) SIGMA(Y) SIGMA(Z)
5.12250877E+000 3.95614450E-001 3.95839691E-001 [arcsec]
-----
PIX2RADX = 7.805500300000E-005[rad/pixel]
XPIXSIZE = 16.1000[arcsec]
PIX2RADY = 7.805500300000E-005[rad/pixel]
YPIXSIZE = 16.1000[arcsec]
CXO = 10.5[pixel] = 169.05[arcsec]
CYO = 2.0[pixel] = 32.20[arcsec]
-----
NOMINAL BETA0 = 2.804741000000E-006[rad/encoder unit]
ENCODER UNIT SIZE = 0.58[arcsec]
GAMMA_E0 = 2007.00[encoder unit] = 1161.09[arcsec]
-----
| -1 | +0 |
FLIP MATRIX D = |---|---| and DG = -1
| +0 | -1 |
-----
```

3.3 IPF EXECUTION LOG

```

*****
IPF EXECUTION-LOG FILE NAME: LG504087.dat
INSTRUMENT TYPE: MIPS_160um_center_large_FOV
IPF FILTER EXECUTION DATE: 04-Dec-2003 TIME: 15:48
IPF FILTER VERSION USED: IPF.V3.0.0B
```

```
*****
----- Loading & Preparing Input Files -----
AAFILE: AA501087 Loaded!          AAFILE dimension = 290002 X 21
ASFFILE: AS501087 Loaded!
CAFFILE: CA502087 Loaded!          CAFFILE dimension = 100 X 15
CBFILE: CB901087 Loaded!          CBFFILE dimension = 178 X 15
CCFILE: CC504087 Created!         CCFILE dimension = 278 X 19
CSFILE: CS502087 Loaded!
Loading Input Files Completed!
-----
----- Selected Mask Vectors -----
index = 1 2 3 4 5 6 7 8 9 10 11 12 13 14 15 16 17 18 19 20
-----
mask1 = [ 1 1 0 0 0 0 0 0 0 0 0 0 0 0 0 0 0 0 0 0 ]
mask2 = [ 1 1 1 1 1 1 1 1 1 1 1 1 1 1 1 1 1 1 1 1 ]
-----
----- Selected Initial Gyro Bias Parameters -----
User Entered 1 : Use AFILE database - from S/C filter
IPF Linearized Using Following Nominal Gyro Bias Estimates
bg0 = [-4.1339711742693908E-007 -2.0063052375007828E-007 +3.6787506019209104E-007 ]
cg0 = [+0.000000000000000E+000 +0.000000000000000E+000 +0.000000000000000E+000 ]
-----
----- Gyro Pre-Processor Run Completed -----
AGFILE CREATED: AG504087.m      ACFILE CREATED: AC504087.m
-----
Total Gyro Preprocessor Execution Time: 87 seconds

FRAME TABLE ENTRIES FOR PCRS LOADED TO TPCRS
q_PCRS4 = [ +5.3371888965461637E-007    q_PCRS5 = [ +7.3379987833742897E-007
            +3.7444233778550031E-004          +5.2236196154513707E-004
            -1.4253684912431913E-003          -1.4047712280184723E-003
            +9.9999891405806784E-001          +9.9999887687698918E-001 ];
q_PCRS8 = [ -5.2779261998836216E-007    q_PCRS9 = [ -7.1963421681856818E-007
            +3.8462959425181312E-004          +5.3239763239987400E-004
            +1.3722087221825403E-003          +1.3516841804518383E-003
            +9.9999898455099423E-001          +9.9999894475050310E-001 ];
-----
----- Initial Conditions for State ----- ----- Initial Square-Root Cov (diag) -----
p1(01) = a00 = +0.000000000000000E+000 Sigma_initial(01,01) = 1.000000000000000E+000
p1(02) = b00 = +0.000000000000000E+000 Sigma_initial(02,02) = 1.000000000000000E+000
p1(03) = c00 = +0.000000000000000E+000 Sigma_initial(03,03) = 9.999900000000000E+004
p1(04) = a10 = +0.000000000000000E+000 Sigma_initial(04,04) = 9.999900000000000E+004
p1(05) = b10 = +0.000000000000000E+000 Sigma_initial(05,05) = 9.999900000000000E+004
p1(06) = c10 = +0.000000000000000E+000 Sigma_initial(06,06) = 9.999900000000000E+004
p1(07) = d10 = +0.000000000000000E+000 Sigma_initial(07,07) = 9.999900000000000E+004
p1(08) = a20 = +0.000000000000000E+000 Sigma_initial(08,08) = 9.999900000000000E+004
p1(09) = b20 = +0.000000000000000E+000 Sigma_initial(09,09) = 9.999900000000000E+004
p1(10) = c20 = +0.000000000000000E+000 Sigma_initial(10,10) = 9.999900000000000E+004
p1(11) = d20 = +0.000000000000000E+000 Sigma_initial(11,11) = 9.999900000000000E+004
p1(12) = a01 = +0.000000000000000E+000 Sigma_initial(12,12) = 9.999900000000000E+004
p1(13) = b01 = +0.000000000000000E+000 Sigma_initial(13,13) = 9.999900000000000E+004
p1(14) = c01 = +0.000000000000000E+000 Sigma_initial(14,14) = 9.999900000000000E+004
p1(15) = d01 = +0.000000000000000E+000 Sigma_initial(15,15) = 9.999900000000000E+004
p1(16) = e01 = +0.000000000000000E+000 Sigma_initial(16,16) = 9.999900000000000E+004
p1(17) = f01 = +0.000000000000000E+000 Sigma_initial(17,17) = 9.999900000000000E+004
-----
p2f(01) = am1 = +0.000000000000000E+000 Sigma_initial(18,18) = 1.000000000000001E-001
p2f(02) = am2 = +0.000000000000000E+000 Sigma_initial(19,19) = 1.000000000000001E-001
p2f(03) = am3 = +1.000000000000000E+000
p2f(04) = beta = +1.000000000000000E+000
```

```

p2f(05) = qT1 = -1.8265322546296804E-006 Sigma_initial(20,20) = 1.00000000000000001E-001
p2f(06) = qT2 = -1.0686509308528702E-003 Sigma_initial(21,21) = 1.0000000000000000E-002
p2f(07) = aT3 = -1.7606843785389105E-003 Sigma_initial(22,22) = 1.0000000000000000E-002
p2f(08) = qT4 = +9.9999787898393622E-001
p2f(09) = qR1 = +7.1086635580286384E-004 Sigma_initial(23,23) = 2.4834623338276731E-004
p2f(10) = qR2 = +1.2695571640506387E-003 Sigma_initial(24,24) = 1.9179929772025390E-005
p2f(11) = qR3 = -1.6159859660547227E-004 Sigma_initial(25,25) = 1.9190849786804107E-005
p2f(12) = qR4 = +9.9999892711639404E-001
p2f(13) = brx = +0.0000000000000000E+000 Sigma_initial(26,26) = 3.6506876102645698E-005
p2f(14) = bry = +0.0000000000000000E+000 Sigma_initial(27,27) = 3.6506876102645698E-005
p2f(15) = brz = +0.0000000000000000E+000 Sigma_initial(28,28) = 3.6506876102645698E-005
p2f(16) = crx = +0.0000000000000000E+000 Sigma_initial(29,29) = 1.3327520027739235E-009
p2f(17) = cry = +0.0000000000000000E+000 Sigma_initial(30,30) = 1.3327520027739235E-009
p2f(18) = crz = +0.0000000000000000E+000 Sigma_initial(31,31) = 1.3327520027739235E-009
p2f(19) = bgx = +0.0000000000000000E+000 Sigma_initial(32,32) = 3.6506876102645698E-005
p2f(20) = bgy = +0.0000000000000000E+000 Sigma_initial(33,33) = 3.6506876102645698E-005
p2f(21) = bgz = +0.0000000000000000E+000 Sigma_initial(34,34) = 3.6506876102645698E-005
p2f(22) = cgx = +0.0000000000000000E+000 Sigma_initial(35,35) = 1.3327520027739235E-009
p2f(23) = cgy = +0.0000000000000000E+000 Sigma_initial(36,36) = 1.3327520027739235E-009
p2f(24) = cgz = +0.0000000000000000E+000 Sigma_initial(37,37) = 1.3327520027739235E-009
-----
```

```

----- IPF KALMAN FILTER STARTED -----
Iteration#001: |dp|= +2.909048200817E-001 RMS(|Res|)=+3.586041228166E-005
Iteration#002: |dp|= +1.906579468450E-002 RMS(|Res|)=+1.513473029503E-005
Iteration#003: |dp|= +6.749589167360E-003 RMS(|Res|)=+1.442297527933E-005
Iteration#004: |dp|= +1.651131361828E-003 RMS(|Res|)=+1.442381898819E-005
Iteration#005: |dp|= +2.702320968600E-004 RMS(|Res|)=+1.441138516578E-005
Iteration#006: |dp|= +1.578603291773E-004 RMS(|Res|)=+1.441033538454E-005
Iteration#007: |dp|= +9.414198609905E-006 RMS(|Res|)=+1.441104029507E-005
Iteration#008: |dp|= +1.173222183905E-005 RMS(|Res|)=+1.441104525341E-005
Iteration#009: |dp|= +1.381831173267E-006 RMS(|Res|)=+1.441099087491E-005
Iteration#010: |dp|= +7.560111465251E-007 RMS(|Res|)=+1.441099663963E-005
Iteration#011: |dp|= +1.725440187165E-007 RMS(|Res|)=+1.441100005744E-005
Iteration#012: |dp|= +3.878416850144E-008 RMS(|Res|)=+1.441099925839E-005
Iteration#013: |dp|= +1.64911212435E-008 RMS(|Res|)=+1.441099909325E-005
Iteration#014: |dp|= +1.367417547584E-009 RMS(|Res|)=+1.441099917077E-005
Iteration#015: |dp|= +1.324143167151E-009 RMS(|Res|)=+1.441099917452E-005
Iteration#016: |dp|= +1.115896350362E-010 RMS(|Res|)=+1.441099916836E-005
Iteration#017: |dp|= +9.056983725984E-011 RMS(|Res|)=+1.441099916876E-005
Iteration#018: |dp|= +1.620171494363E-011 RMS(|Res|)=+1.441099916917E-005
Iteration#019: |dp|= +5.771602829998E-012 RMS(|Res|)=+1.441099916911E-005
Iteration#020: |dp|= +2.723996166162E-012 RMS(|Res|)=+1.441099916907E-005
Iteration#021: |dp|= +1.928934671741E-012 RMS(|Res|)=+1.441099916910E-005
Iteration#022: |dp|= +4.608870405026E-013 RMS(|Res|)=+1.441099916909E-005
Iteration#023: |dp|= +1.049857617017E-012 RMS(|Res|)=+1.441099916908E-005
Iteration#024: |dp|= +2.182186934455E-012 RMS(|Res|)=+1.441099916908E-005
Iteration#025: |dp|= +3.506475805329E-012 RMS(|Res|)=+1.441099916909E-005
Iteration#026: |dp|= +1.393865431942E-012 RMS(|Res|)=+1.441099916908E-005
Iteration#027: |dp|= +9.939072741653E-013 RMS(|Res|)=+1.441099916907E-005
Iteration#028: |dp|= +5.109500163929E-013 RMS(|Res|)=+1.441099916909E-005
Iteration#029: |dp|= +1.079780068300E-012 RMS(|Res|)=+1.441099916909E-005
Iteration#030: |dp|= +3.001894601360E-013 RMS(|Res|)=+1.441099916908E-005
IPF Kalman Filter Completed with Error |dp1| + |dp2| = +3.0018946013595259E-013
-----
```

```

----- IPF LEAST SQUARES FILTER STARTED -----
Iteration#001 COND#=+3.449403235295E+008, |dp|=+2.931488978539E-001
Iteration#002 COND#=+3.449406061470E+008, |dp|=+2.319482142443E-002
Iteration#003 COND#=+3.449303718802E+008, |dp|=+1.328898565591E-003
Iteration#004 COND#=+3.449295965280E+008, |dp|=+6.730891738446E-005
Iteration#005 COND#=+3.449296336697E+008, |dp|=+1.860409625760E-006
Iteration#006 COND#=+3.449296321319E+008, |dp|=+4.867938278461E-008
Iteration#007 COND#=+3.449296316845E+008, |dp|=+1.277404455160E-009
```

```

Iteration#008 COND#=+3.449296318298E+008, |dp|=+3.453089992996E-011
Iteration#009 COND#=+3.449296322908E+008, |dp|=+1.693533102817E-012
Iteration#010 COND#=+3.449296317049E+008, |dp|=+9.924783351334E-013
Iteration#011 COND#=+3.449296320448E+008, |dp|=+1.686433560297E-012
Iteration#012 COND#=+3.449296313519E+008, |dp|=+1.064894538061E-012
Iteration#013 COND#=+3.449296323951E+008, |dp|=+7.762060577230E-013
Iteration#014 COND#=+3.449296321660E+008, |dp|=+2.209285922341E-012
Iteration#015 COND#=+3.449296321189E+008, |dp|=+8.034779224187E-013
Iteration#016 COND#=+3.449296321208E+008, |dp|=+2.464037603347E-013
Iteration#017 COND#=+3.449296317871E+008, |dp|=+1.326385840703E-012
Iteration#018 COND#=+3.449296313913E+008, |dp|=+7.540272920896E-013
Iteration#019 COND#=+3.449296322698E+008, |dp|=+2.338486189412E-013
Iteration#020 COND#=+3.449296321956E+008, |dp|=+1.063011636465E-012
Iteration#021 COND#=+3.449296319696E+008, |dp|=+1.117315410601E-012
Iteration#022 COND#=+3.449296324075E+008, |dp|=+2.254721343162E-013
Iteration#023 COND#=+3.449296318224E+008, |dp|=+4.264499532767E-013
Iteration#024 COND#=+3.449296325113E+008, |dp|=+7.240992097472E-013
Iteration#025 COND#=+3.449296325063E+008, |dp|=+8.154622880402E-013
Iteration#026 COND#=+3.449296321686E+008, |dp|=+6.435759403182E-013
Iteration#027 COND#=+3.449296319108E+008, |dp|=+7.643937444252E-013
Iteration#028 COND#=+3.449296317808E+008, |dp|=+5.790012147928E-013
Iteration#029 COND#=+3.449296323159E+008, |dp|=+6.696247838698E-013
Iteration#030 COND#=+3.449296320639E+008, |dp|=+6.207281461493E-013
IPF Least Squares Filter Completed with Error |dp1| + |dp2| = +6.2072814614926934E-013
-----
```

Total Execution Time: 910 seconds

4 COMMENTS

This run (ID504087) is a re-run of the earlier 160um fine survey (ID502087) using an improved set of science centroids that we retrieved from DOM as CA502087. The centroids were re-centroided by the MIPS Team using a more sophisticated algorithm. The results of this run are summarized as follows:

1. The initial delivered data sets (CA502087 and CB502087) contained 100 MIPS science centroids and 180 PCRS centroids.
2. A 45 minute segment of attitude history data was missing in the AA file. Consequently, the first sandwich maneuver (at about 4.7 hours into the experiment) was removed because the GCF correction associated with this data was corrupted.
3. We estimated a total of 22 parameters: 2 plate scales (in V and W), 2 scan mirror, 3 Brown angles for the prime frame, 3 STA to TPF alignment, 6 thermo-mechanical induced drift, and 6 gyro drift bias parameters.
4. The plate scale for the V direction was found to be 21 Although somewhat large, it was decided to keep them after consultation with the MIPS science team.

Aside from the large plate scale issue discussed above, we recommend Frame Table changes for frames 87, 88, 89, 91 and 92 as given in the IF file IF504087.dat for FTU#15. The recommended changes are on order of: 0.36" in Y, 5.3" in Z and 0.38 deg in X for the prime frame 87. These estimates are expected to be accurate to 0.37" and meet the fine survey pointing requirement of 3.7". Note that the 160 um Fine Survey will be revisited in future runs supporting FTU#16.

IPF TEAM CONTACT INFORMATION

IPF Team email	ipf@sirtfweb.jpl.nasa.gov	
David S. Bayard	X4-8208	David.S.Bayard@jpl.nasa.gov (TEAM LEADER)
Dhemetrio Boussalis	X4-3977	boussali@grover.jpl.nasa.gov
Paul Brugarolas	X4-9243	Paul.Brugarolas@jpl.nasa.gov
Bryan H. Kang	X4-0541	Bryan.H.Kang@jpl.nasa.gov
Edward.C.Wong	X4-3053	Edward.C.Wong@jpl.nasa.gov (TASK MANAGER)

ACKNOWLEDGEMENTS

This work was performed at the Jet Propulsion Laboratory, California Institute of Technology, under contract with the National Aeronautics and Space Administration.

References

- [1] D.S. Bayard, B.H. Kang, *SIRTF Instrument Pointing Frame Kalman Filter Algorithm*, JPL D-Document D-24809, September 30, 2003.
- [2] B.H. Kang, D.S. Bayard, *SIRTF Instrument Pointing Frame (IPF) Software Description Document and User's Guide*, JPL D-Document D-24808, September 30, 2003.
- [3] D.S. Bayard, B.H. Kang, *SIRTF Instrument Pointing Frame (IPF) Kalman Filter Unit Test Report*, JPL D-Document D-24810, September 30, 2003.
- [4] *Space Infrared Telescope Facility In-Orbit Checkout and Science Verification Mission Plan*, JPL D-Document D-22622, 674-FE-301 Version 1.4, February 8, 2002.
- [5] *Space Infrared Telescope Facility Observatory Description Document*, Lockheed Martin LMMS/P458569, 674-SEIT-300 Version 1.2, November 1, 2002.
- [6] *SIRTF Software Interface Specification for Science Centroid INPUT Files (CAFILER, CSFILE)*, JPL SOS-SIS-2002, November 18, 2002.
- [7] *SIRTF Software Interface Specification for Inferred Frames Offset INPUT Files (OFILE)*, JPL SOS-SIS-2003, November 18, 2002.
- [8] *SIRTF Software Interface Specification for PCRS Centroid INPUT Files (CBFILE)*, JPL SIS-FES-015, November 18, 2002.
- [9] *SIRTF Software Interface Specification for Attitude INPUT Files (AFILE, ASFILE)*, JPL SIS-FES-014, January 7, 2002.
- [10] *SIRTF Software Interface Specification for IPF Filter Output Files (IFFILE, LGFILE, TARFILE)*, JPL SOS-SIS-2005, November 18, 2002.
- [11] R.J. Brown, *Focal Surface to Object Space Field of View Conversion*. Systems Engineering Report SER No. S20447-OPT-051, Ball Aerospace & Technologies Corp., November 23, 1999.